ANNALS OF PHYSICS: 66, 578–623 (1971)

Partons and Their Applications at High Energies*

SIDNEY D. DRELL AND TUNG-MOW YAN†

Stanford Linear Accelerator Center,
Stanford University, Stanford, California 94305

Received October 2, 1970

DEDICATION

This paper is dedicated to the memory of Amos de-Shalit, with deep sadness at the loss, not only of a very distinguished and important scientific colleague, but also of a very close personal friend whose gentleness was matched only by his wisdom. In his tragically brief life he persistently strove to bridge the growing gulfs between different scientific disciplines as also between different cultures and nations. Of special physical interest to him was the unity of concepts in nuclear and particle physics, an example of which is presented here in the form of the impulse approximation.

S.D.D.

We discuss Feynman's parton model for deep inelastic weak or electromagnetic processes as an application of the impulse approximation to elementary particle interactions. The special features and conditions permitting this application are elaborated upon in some detail including the dependence of the parton model and the impulse treatment on an appropriate choice of coordinate frames and the role of the very soft or "wee" partons. Application of the parton model is made to the calculation of the cross section for massive lepton pair production in very high energy hadron–hadron collisions and compared with experiment. The conjectured role of light cone singularities in describing this and the other deep inelastic amplitudes is also discussed.

I. PARTONS AND THE IMPULSE APPROXIMATION

We discuss Feynman's parton model [1] for deep inelastic weak or electromagnetic processes as an application of the impulse approximation to elementary particle interactions. The special features and conditions permitting this application of the impulse approximation, whose roots lie in the nonrelativistic domain of

* Work supported by the U. S. Atomic Energy Commission.

† Present address: Laboratory of Nuclear Studies, Cornell University, Ithaca, New York 14850.

atomic and nuclear bound states, to particle physics are elaborated upon in some detail. In particular we investigate by specific calculation the dependence of the parton model and the impulse treatment on an appropriate choice of coordinate frames and the role of the very soft or "wee" partons. We also present a more complete discussion of the application of the parton model to the calculation of the cross section for massive lepton pair production in very high energy hadron–hadron collisions [2]. The conjectured role of light cone singularities in describing this and the other deep inelastic amplitudes is also discussed and criticized.

In order to apply the impulse approximation we demand the following [1,3]. We analyze the bound system—be it a nucleon or nucleus—in terms of its constituents, called "partons." Nucleons are the "partons" of the nucleus, and the "partons" of a nucleon itself are still to be deciphered though we may wish to call them quarks in that (a) they have a heuristic value in serving as additive constituents in appropriate reference frames, and (b) their existence has not been confirmed definitively by direct observation. If we specify the kinematics so that the partons can be treated as instantaneously free during the duration of a sudden pulse carrying a large energy transfer from the projectile or from some external current, then we can neglect their binding effects during the interaction and we can treat the kinematics of the collision as between two free particles, a projectile and the parton. With these conditions the impulse approximation applies.

There is a big difference between the kinematical regime that fulfills the conditions for applying the impulse approximation to protons from those for applying it to nuclei or atoms. This is because the latter, in contrast to a nucleon itself, are structures made up of weakly bound and well identified individual nucleons or electrons. Thus the ratio of binding energies to rest energies for the constituents are typically

$$\text{for an atom} \qquad \frac{\text{few eV}}{0.51\ \text{MeV}} \sim 10^{-5} \ll 1,$$

$$\text{for a nucleus} \qquad \frac{8\ \text{MeV}}{938\ \text{MeV}} \sim 10^{-2} \ll 1,$$

$$\text{for a proton} \qquad \frac{\text{100's of MeV}}{\text{100's of MeV}} \sim 1.$$

The Bjorken [4] deep inelastic limiting region satisfies the condition for applying an impulse approximation [1] to the electron scattering from protons as viewed from a certain class of $P \to \infty$, or infinite momentum frames. The "partons" constituting a proton are strongly bound together as viewed in the rest frame. However if their bound state can be formed by momentum components that are limited in magnitude below some fixed maximum—i.e., if there exists a *finite* $k_{\max}$—then as viewed in an infinite momentum frame the partons will each share

a finite fraction $0 < x_i < 1$ of the infinite momentum P along the three-axis. These parton states are long lived by virtue of the time dilation as characterized by

$$\tau_{\text{life}} \sim \frac{1}{\sum_i \sqrt{x_i^2 P^2 + k_{i\perp}^2 + M_i^2} - \sqrt{P^2 + M^2}}$$

$$\approx \frac{2P}{\sum_i \frac{k_{i\perp}^2 + M_i^2}{x_i} - M^2} \equiv \frac{P}{M_{\text{eff}}^2}, \tag{1}$$

where $k_{i\perp}$, M_i, and x_i are, respectively, the transverse momentum, rest mass, and fraction of P carried by each parton: $\sum_i x_i = 1$. The derivation of this intuitively appealing picture from a canonical quantum field theory [5] modified by imposing a maximum constraint on $k_\perp$, and its applicability to a particular class of amplitudes, has been discussed. Equation (1) exhibits the increase in lifetime by the relativistic factor P/M_{eff} of a virtual state of mass M_{eff} formed with lifetime $1/\Delta E \sim 1/M_{\text{eff}}$ as viewed in a rest frame.

For finite values of the fractional longitudinal momenta x_i this lifetime τ_{life} is long compared with the duration of the pulse, τ_{int}, from the inelastically scattered electron in the deep inelastic region. In the electron–proton collision center-of-mass system the latter is given by

$$\tau_{\text{int}} \sim \frac{1}{q_0} = \frac{4P}{2M\nu - Q^2} = \frac{2P}{M\nu}\left(\frac{\omega}{\omega - 1}\right); \qquad \omega \equiv \frac{2M\nu}{Q^2} > 1, \tag{2}$$

and hence we see that $\tau_{\text{int}} \ll \tau_{\text{life}}$ provided

$$2M\nu - Q^2 = 2M\nu\left(1 - \frac{1}{\omega}\right) \gg M_{\text{eff}}^2. \tag{3}$$

For this condition to be satisfied we need in (1) both a bound on $k_{\perp\max}^2$ and a restriction preventing x from approaching within M^2/Q^2 or M/ν of its end point values. The requirement to satisfy this latter condition is that we work in the Bjorken limiting region of kinematics for this process where $2M\nu$, $Q^2 \gg M^2$ and the ratio of the large energy and momentum transfers, ω, is finite. Then the fraction x of longitudinal momentum on the parton from which the electron scatters is also finite and restricted from its end point values since, as first shown by Feynman [1], it is given by $x = (1/\omega)$. Moreover in this kinematic regime the interaction with the long-lived parton, which is essentially free by (3), conserves energy as well as momentum across the interaction vertex with the electron in Fig. 1. We have thus satisfied the conditions for applying an impulse approximation.

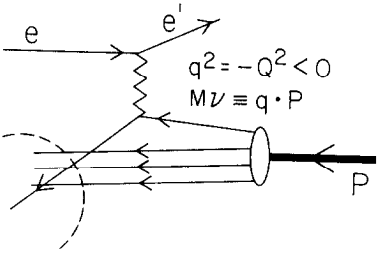

FIG. 1. Inelastic electron–proton scattering viewed in the $P \to \infty$ frame.

If we want to find other processes which satisfy the same kinematical constraints and allow application of the impulse picture of "partons" in an infinite momentum frame we need look for interactions at high energies s which absorb or produce a lepton system of huge mass Q^2 such that the ratio Q^2/s is finite. We confine our attention here to massive lepton systems which can be safely treated by perturbation theory in the electromagnetic or weak couplings although, by further extending the assumptions for the theoretical framework, massive hadron systems could be included in the same kinematical framework just as well. Beyond the deep inelastic neutrino processes and electron–positron annihilation cross sections: $\nu + p \to e + \cdots$, and $e + e^- \to$ hadron $+ \cdots$ which have already been discussed and analyzed [5] an additional observable cross section that meets the conditions for applying an impulse analysis [2] is

$$p + p \to (\mu\bar{\mu}) + \cdots \tag{4}$$

Preliminary measurements of this process have been reported [6].

The organization of this paper is as follows. A more detailed discussion of the kinematical conditions for processes in which the interaction can be described using the impulse approximation in terms of hard partons in contrast to those in which the wee partons are predominant is presented in Section II. In Section III we analyze the dependence of our parton model picture on the appropriate choice of infinite momentum ($P \to \infty$) coordinate frames. Section IV is devoted to showing that general scaling predictions of the parton model, or the impulse approximation, are not altered by the wee partons. In Section V we study the cross section (4) for massive lepton pair production by hadrons at high energy deriving its scaling properties and the parton model for finite Q^2/s. Finally in Section VI we analyze briefly the significance of the behavior of the product of current operators near the light cone for the deep inelastic processes we have studied with the parton model.

II. Wee Versus Hard Partons

In contrast to processes such as (4) which meet the requirements for the impulse approximation and can be described in terms of partons, let us turn next to the conjectured role of the parton model in describing the predominant hadron–hadron interactions. These processes include pp and πp elastic, resonance excitation, or total "inclusive" cross sections, and may best be viewed in the collision center-of-mass system. Then we can picture two colliding hadrons with very high momenta P, such that $s = 4P^2$, one moving to the right and one to the left. How do they interact? What is exchanged between the two lines in Fig. 2? It is not the "hard partons" which share a finite fraction of the individual nucleons' P and therefore retain their sense of heading to the right or the left respectively. In order to insert a right moving hard parton into a left running proton state one pays a penalty of a factor $1/s$ as computed directly from energy denominators such as in (1). This is the price to introduce a relative momentum of magnitude $2P$ into the wavefunction of a ground state built predominantly from finite momentum components which we take to be our working hypothesis. Rather it is the "soft" or "wee" partons of Feynman that bear only a finite momentum—or a "wee" fraction of P—and are equally at home on the right as on the left moving line that are exchanged [1]. In contrast to the hard partons responsible for the scaling in the deep inelastic processes and whose momentum distribution is measured in those experiments, it is the wee partons that determine the hadron–hadron cross sections. As described by Feynman, "wee" means that the partons carry less than or up to typically 1 GeV momentum or a fraction $x \sim 1$ GeV$/P$ of the proton momentum. In that a mass $\sim$1 GeV is introduced, scale invariance no longer applies to this analysis; and this is as it must be if total hadronic cross sections approach constant values (to within logarithmic factors) as their high energy limiting behavior, so that $\sigma_{\text{tot}} \sim M^{-2}$. If scaling remained valid the only dimension would be $\sigma_{\text{tot}} \sim (1/s) \to 0$ as $s \to \infty$.

Feynman [1] has postulated a specific spectrum for the soft or "wee" parton distribution. His argument is that since these "wee" partons with $x \sim (1 \text{ GeV}/\sqrt{s})$ are responsible for the hadronic cross sections, their momentum spectrum must be

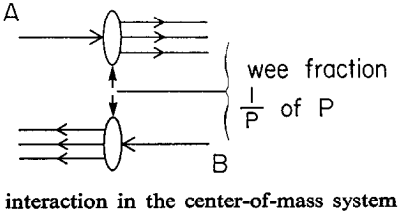

FIG. 2. Hadron–hadron interaction in the center-of-mass system at high energy via "wee" parton exchange.

consistent with the observed (to within logarithmic factors) constant total cross sections at very high energies. Thus if the amplitude to emit or absorb a "wee" parton in a momentum interval dx about x is given by (dx/x^{α}) we find the total hadronic cross section can be expressed by

$$\sigma_{\text{tot}} \sim \left\{\int^{C/E_a} \frac{dx_a}{x_a{}^{\alpha}}\right\}^2 \left\{\int^{C/E_b} \frac{dx_b}{x_b{}^{\alpha}}\right\}^2 \sim (E_a E_b)^{2(\alpha-1)} \sim s^{2(\alpha-1)},$$

and therefore $\alpha = 1$. However it should be recognized that independent of the success or failure of this extrapolation into the wee region, the concept of partons for the deep inelastic scaling region in which the impulse approximation applies and each constituent contributes incoherently as shown in [5, Paper II] is to be judged on its own merits. Indeed its theoretical base is more firm.

What we would like to emphasize next is that the situation is very different for hadron–hadron interactions when we are dealing with processes such as (4) in which massive systems are created. If the massive pair emerges by bremsstrahlung from one of the nucleon lines the interaction cannot proceed via "wee" exchanges only. This is kinematically impossible when we satisfy the constraints of energy—momentum conservation for the overall process.

We can illustrate this in two different coordinate systems that emphasize different aspects of the problem. To prove this consider first the kinematics in the collision center-of-mass system with the momentum labels of Fig. 3 which show two incident hadrons scattering to produce two final hadronic systems plus a pair of very large mass Q^2. Since the masses as well as the transverse momenta of the hadronic systems (A) and (B) are negligible relative to the energy of each colliding nucleon, $\frac{1}{2}\sqrt{s}$, and to the lepton pair mass $\sqrt{Q^2} \sim \sqrt{s}$, we can neglect them for simplicity, writing the statement of energy conservation as

$$\sqrt{s} = \sqrt{x^2 \frac{s}{4} + q_{\perp}{}^2 + Q^2} + (1 - x - x')\frac{1}{2}\sqrt{s} + (1 - x')\frac{1}{2}\sqrt{s} \qquad (5)$$

as shown in Fig. 3. $x < 1$ is the fraction of the right moving momentum transferred to a massive pair it produces (by bremsstrahlung) and we make no assumption on its magnitude; x' is the fraction of $\frac{1}{2}\sqrt{s}$ transferred by the left moving hadron. Solving (5) for the transferred momentum we find

$$x' = \frac{1}{2}\left[\sqrt{x^2 + 4\frac{q_{\perp}{}^2 + Q^2}{s}} - x\right]. \qquad (6)$$

For finite Q^2/s, x' is a finite fraction according to (6); thus the exchanged momentum is given by $x'P \sim \sqrt{s}$. This then does not describe interchange of only "wee"

or very soft partons between the nucleons, but rather of hard ones with a finite fraction of P.

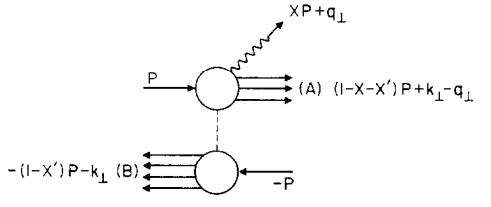

FIG. 3. Kinematics for massive lepton pair production by bremsstrahlung from on of the nucleon lines.

In contrast if we consider ordinary hadron cross sections with only finite mass particles appearing in the final state and with limited transverse momenta so that in (6) $[q_\perp{}^2 + Q^2]$ is replaced by a finite mass M_{eff}^2, we have

$$x' \sim M_{\text{eff}}^2/s \qquad \text{for} \quad 1 > x \gg M_{\text{eff}}/\sqrt{s}; \tag{7a}$$

$$x' \sim M_{\text{eff}}/\sqrt{s} \qquad \text{for} \quad x \lesssim M_{\text{eff}}/\sqrt{s} \tag{7b}$$

The significance of (7) is this: for inelastic hadron processes leading to soft final particles, viz., processes including "pionization" so that final particles are produced with limited, finite energies in the center-of-mass frame; i.e., with energies, $x\sqrt{s} \approx M_{\text{eff}}$ (7b) applies. Then the interaction can take place with wee parton exchange, i.e., with a momentum exchange in Fig. 2 between the hadron lines of order $x'\sqrt{s} \sim M_{\text{eff}}$ as suggested by Feynman.

This is in contrast with both elastic two-body high energy processes as well as with inelastic ones that exclude pionization, or a soft hadron component, in the center-of-mass system. In these cases, by (7a), the final x are finite and the exchanged momentum is characterized by $x' \sim M_{\text{eff}}^2/s$ so that the exchanged momentum is $x'\sqrt{s} \sim M_{\text{eff}}^2/\sqrt{s}$, i.e., it is "super wee." Thus there are *three* distinct regions to consider in describing the high energy hadron interactions: those relying on hard partons (H), wee partons (W), and super-wee parton (sW). The hard partons enter processes involving an external line bearing a very large mass; wee partons are exchanged in ordinary hadron processes leading to pionization, or a soft component of final particles in the center-of-mass system; and super-wee ones enter elastic processes, or those from which a soft final component is excluded.

In terms of "collision times" in the center-of-mass frame, hard parton exchange occurs during the vanishingly small interval $\tau_{\text{H}} \sim 1/xP \sim 1/x\sqrt{s} \sim 1/\sqrt{s}$; "wee"

exchanges leading to a constant high energy cross section occur during a finite interval $\tau_W \sim 1/x\sqrt{s} \sim 1/M_{\text{eff}}$; and a super wee one has an increasing interval of coherence $\tau_{SW} \sim \sqrt{s}/M_{\text{eff}}^2$.

In terms of an intuitive wavefunction picture of a hadron as a bound system one may characterize these regions as follows. The loosely bound constituents of the proton as viewed in the rest frame will generally acquire a finite fraction of the infinite momentum P in a Lorentz transformation, or boost, to an infinite momentum frame. These are the hard partons and their distribution can be analyzed in the impulse approximation and is probed by deep inelastic processes in the Bjorken region of finite ω, or with finite Q^2/s. One begins to probe into the wee region, characterized by very high momentum components in the rest frame, as one moves out to extreme values of ω. Thus in the deep inelastic electron scattering cross section, for $\omega \gg 1$ the electron scatters from a soft-to-wee parton with a fraction $x = 1/\omega \ll 1$ of the proton's longitudinal momentum. Also as we approach the threshold $\omega \sim 1$ the scattering is from a parton with all but a fraction $(1 - 1/\omega)$ of the momentum and as this fraction decreases into the wee region the probability of such partons existing is also being probed [7]. As one enters into the wee region the conditions for Bjorken scaling are violated and a scale length such as a mass M or transverse momentum cutoff $k_{\perp \max}$ enters the problem. Finally for elastic processes, as well as inelastic events excluding a soft final component, we have the super wee region. By unitarity, or simply the optical theorem, the elastic and inelastic amplitudes are coupled nonlinearly. This tells us that what we have called the "super wee" region is necessarily related to the "wee" one that plays the major role in inelastic hadronic processes. This connection is illustrated in Fig. 4 which shows that one or more closed loops of wee exchanges can after cancellation of the momenta carried by the individual partons lead to a net transfer of super-wee momentum. Thus all super-wee effects may be no more than a reflection of

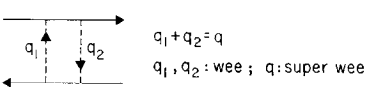

FIG. 4. Example of a super wee exchange as a result of super position of two wee exchanges.

multiple wee exchanges. However we cannot say the same for a relation between hard and wee partons. The wee parton effects cannot be mocked up by a multiple exchange of hard partons as we now show. For this, it is more convenient to use a true infinite momentum system, i.e., one with $P \to \infty$, and with *large but fixed s* and Q^2. Let us therefore boost ourselves into such a frame.

We define our infinite momentum frame by Lorentz transformation to a moving coordinate frame with velocity β down along the vertical axis in Fig. 2. The resulting kinematics are shown in Fig. 5. Dropping finite masses in the high energy

limit, $s/M^2 \gg 1$, we can write for the energy-momentum four vectors of the two incident hadrons

$$P_1 : \left(P + \frac{s}{8P}, 0, P, \frac{1}{2}\sqrt{s}\right),$$
$$P_2 : \left(P + \frac{s}{8P}, 0, P, -\frac{1}{2}\sqrt{s}\right), \tag{8}$$

where

$$\frac{\beta}{\sqrt{1-\beta^2}} = 2P/\sqrt{s} \quad \text{or} \quad \beta \approx 1 - s/8P^2.$$

The final hadron in Fig. 3 with center-of-mass momentum components $-\frac{1}{2}(1-x')\sqrt{s}$ and $-k_\perp$ parallel and perpendicular, respectively, to the collision axis is boosted in this system to one with components that to leading order are $(1-x')P$ and $-\frac{1}{2}(1-x')\sqrt{s}$ along the direction of the boost and transverse to it, respectively. Thus the momentum transfer from the nucleon line is

$$\mathbf{P}_2 - \mathbf{P}_2' = x'P\hat{\mathbf{i}}_\parallel - \tfrac{1}{2}x'\sqrt{s}\,\hat{\mathbf{i}}_\perp, \tag{9}$$

where $\hat{\mathbf{i}}_\parallel$ and $\hat{\mathbf{i}}_\perp$ denote unit vectors parallel and perpendicular to the direction of the boost.

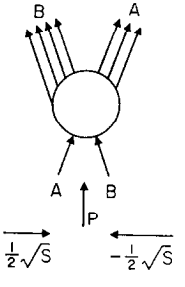

FIG. 5. Hadron–hadron interaction viewed in a true infinite momentum frame with a large transverse momentum mismatch between the two initial hadrons.

In terms of the parton model, (9) together with (6) and (7) reveal the following: For a hadron–hadron collision leading to production of a massive system with mass Q^2 from one of the lines, so that x' is finite as in 6), there *must* be a very large transverse momentum transfer $\sim\sqrt{s}$ between the hadron lines. On the other hand this transverse momentum transfer can be limited to a finite value if wee (or super wee) partons are exchanged in ordinary hadron–hadron collisions as in (7) .Thus if we consider the parton models in an infinite momentum frame as described by (8) and with a finite bound on the transverse momentum components as implied,

or enforced, in the various models that have received detailed study and have provided a base for deriving the Bjorken scaling behavior [5], only the wee partons in the sense of (7a) or (7b) can be exchanged. These will provide the interaction mechanism for the predominant hadronic cross sections. However an exchange of a hard parton as required kinematically for the production of a massive pair state cannot occur under the assumption of a finite limit, $k_{\perp \max}$, at the hadron vertices. Hard partons thus cannot by multiple exchanges simulate wee parton effects, either.

Clearly then the process (4) will not be related to the total nucleon–nucleon cross sections and indeed cannot proceed by the illustrated mechanism in Fig. 3. In other words the massive pair is not produced by bremsstrahlung from one of the nucleon lines. The mechanism for creating the pair that meets all kinematic constraints as well as the condition of limited finite momentum transfer is illustrated in Fig. 6: the pair is created via parton–antiparton annihilation. Viewed from the center-of-mass frame a hard parton moving to the right annihilates on a similar antiparton headed to the left (or vice versa) and the resulting system is very massive since the parton–antiparton energies add while their momenta subtract. From our infinite momentum frame the high energy parton–antiparton pair with parallel longitudinal momenta along **P** but with antiparallel transverse momenta annihilate at the bare electromagnetic vertex to form a pair of mass

$$Q^2 \cong x_1 x_2 s, \tag{10}$$

where x_1 and x_2 are the fractions of their respective proton momenta they are carrying. Equation (10) is a scalar and is most readily derived in the center-of-mass system:

$$\begin{aligned} Q^2 &= (E_1 + E_2)^2 - (\mathbf{P}_1 + \mathbf{P}_2)^2, \\ &\cong (x_1 + x_2)^2 s/4 - (x_1 - x_2)^2 s/4 = x_1 x_2 s. \end{aligned}$$

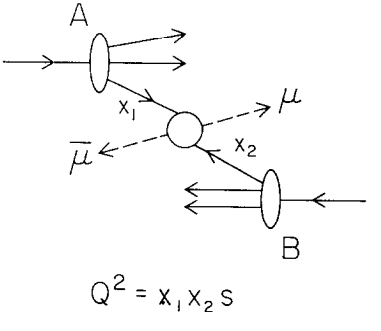

FIG. 6. Production of a massive lepton pair by parton–antiparton annihilation.

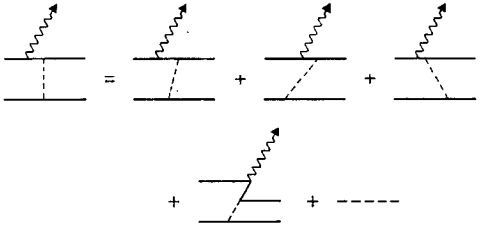

FIG. 7. Example of a covariant Feynman diagram for producing a virtual photon as expressed in terms of a sum of time-ordered old-fashioned perturbation diagrams with both bremsstrahlung and annihilation.

In describing these graphs and amplitudes in this way we are of course not referring to Feynman graphs and amplitudes which combine the annihilation and bremsstrahlung contributions together in covariant mixtures as illustrated in Fig. 7. Our infinite momentum graphs carry a direction of momentum as well as a direction of time as described in our earlier work [5].

In process (4) with finite Q^2/s, (10) shows that one is dealing with hard partons and with the same physical region of parton momenta as probed in the deep inelastic scattering experiments that measure the parton distribution in $x = 1/\omega$. In Section V we present a detailed formal analysis of the theory of this process using the same techniques as presented earlier for the analysis of deep inelastic scattering and pair annihilation. In particular the impulse approximation will be shown to apply and with it the parton model. The discussion of this section was intended to provide the physical picture and intuitive understanding for this development as well as for its relation to other processes.

The ability to construct an impulse approximation treatment for high energy processes with massive external pair states has been a useful step forward in our description and understanding of high energy processes. Tests of these ideas through these and other processes are very important to accomplish, as well as to keep clearly distinct from successes or failures in the wee or super wee regions which are not amenable to an impulse treatment. Indeed the wee regions require extrapolations from the hard parton region along with assumptions on the spectrum of partons. Moreover in general they do not lead to scale invariant results since they contain a cutoff mass or transverse momentum as a parameter.

III. Choice of "Infinite Momentum" Coordinate Systems

Not all infinite momentum frames are suitable for developing a valid parton model picture [8]. The important point to be recognized is that "an infinite momentum frame" is not a Lorentz invariant concept. Neither is the decomposition of an

invariant Feynman amplitude into its separate scattering and pair creation and annihilation parts corresponding to the direction of time on an internal line. As a result, although the use of such infinite momentum frames is essential to the derivation of the parton picture, the specific physical picture does not hold in all of the infinite momentum frames of the nucleon. If the infinite momentum of the nucleon defines the three-axis, i.e., its four-momentum vector is specified by

$$P^\mu = \left(P + \frac{M^2}{2P}, 0, 0, P\right),$$

we must satisfy the defining equations

$$M\nu = +q \cdot P = (q^0 - q_3)\, P + \frac{M^2}{2P}\, q^0\,; \qquad -q^2 = (q_3 + q^0)(q_3 - q^0) + q_\perp{}^2,$$

which require

$$q^0 - q_3 = u/P,$$
$$q^0 = vP,$$

so that both $M\nu$ and q^2 approach a limit independent of P as $P \to \infty$. Two of the simplest choices for u and v are

(a) $v = (2M\nu + q^2)/4P^2$, $u = M\nu$;

in this frame we have

$$q^0 = \frac{2M\nu + q^2}{4P}, \qquad q_3 = -\frac{2M\nu - q^2}{4P}, \qquad -q^2 = q_\perp{}^2 + 0\left(\frac{1}{P^2}\right); \tag{11a}$$

(b) $u = 0, \qquad v = 2\nu/M$;

in this frame we have

$$q = q_3 = \frac{2\nu}{M} P, \qquad -q^2 = q_\perp{}^2. \tag{11b}$$

These two possibilities will be called frame (a) and frame (b), respectively. Frame (a) coincides with the CM system of the incident electron and the target nucleon for electron–proton scattering. These two frames represent the two extreme possibilities for the whole family of infinite momentum frames since in frame (a) both q^0 and q_3 are very small, being of order $1/P$, while in frame (b) both q^0 and q_3 are large, being proportional to P. A variant of frame (a) is $v = 2M\nu/2P^2$, $u = M\nu$, or $q_3 \equiv 0$. By assigning possible values to u and v one obtains the whole family of infinite momentum frames.

The physical picture of the same scattering process has a different appearance in different coordinate systems. To demonstrate this point clearly, we will give as an elementary, almost trivial, example the second-order calculation of the structure functions $W_{1,2}$ in a model of spinless nucleons interacting with spinless pions. This model, though unrealistic, is an ideal example for our purposes because it is super-renormalizable and has thereby the virtue that a Bjorken limit exists in perturbation theory without the need of imposing a high momentum cutoff. The interaction Lagrangian of the model is

$$\mathscr{L}(x) = G\psi^\dagger\psi\phi, \tag{12}$$

where ψ, ϕ are the spinless proton and neutral pion fields, respectively. For simplicity we have omitted additional charge states or isospin families as they can be incorporated without difficulty. The electromagnetic current operator of the model is given by

$$J_\mu(x) = -i\psi^\dagger(x)\,\overleftrightarrow{\partial}_\mu\psi(x). \tag{13}$$

We shall now calculate by three different ways and in different coordinate frames the second-order contribution to the familiar structure functions $W_{1,2}$ in the Bjorken limit. First, these structure functions will be obtained by the frame independent covariant perturbation technique; and then they will be computed in the two infinite momentum frames (a) and (b). The structure functions $W_{1,2}$ are defined as

$$\begin{aligned} W_{\mu\nu} &= 4\pi^2 \frac{E_p}{M} \int (dx)\, e^{+iqx}\langle P \mid J_\mu(x)\, J_\nu(0) \mid P\rangle, \\ &= 4\pi^2 \frac{E_p}{M} \sum_n \langle P \mid J_\mu(0) \mid n\rangle\langle n \mid J_\nu(0) \mid P\rangle(2\pi)^4\, \delta^4(q + P - P_n), \\ &= -\left(g_{\mu\nu} - \frac{q_\mu q_\nu}{q^2}\right) W_1(q^2, \nu) \\ &\quad + \frac{1}{M^2}\left(P_\mu - \frac{P\cdot q}{q^2}\, q_\mu\right)\left(P_\nu - \frac{P\cdot q}{q^2}\, q_\nu\right) W_2(q^2, \nu), \end{aligned} \tag{14}$$

or

$$\begin{aligned} W_1 &= \frac{1}{2(1 - \nu^2/q^2)}\left[-\left(1 - \frac{\nu^2}{q^2}\right) A + B\right], \\ W_2 &= \frac{1}{2(1 - \nu^2/q^2)^2}\left[-\left(1 - \frac{\nu^2}{q^2}\right) A + 3B\right], \end{aligned} \tag{15}$$

where

$$A = W^\mu_\mu, \qquad B = \frac{1}{M^2} P^\mu W_{\mu\nu} P^\nu. \tag{16}$$

The second-order contribution corresponds to the electroproduction of a single pion. This is represented by the three Feynman diagrams in Fig. 8. The covariant calculation follows standard procedures. The gauge invariant tensor $W_{\mu\nu}$ corresponding to Fig. 8 is given by

$$W_{\mu\nu} = \frac{G^2}{(2\pi)^3}\frac{1}{2M}\int \frac{d^3P_1}{2E_1}\frac{d^3k_1}{2\omega_1}\,\delta^4(q + P - P_1 - k_1)\left\{\frac{(2P_\mu + q_\mu)(2P_\nu + q_\nu)}{(2M\nu + q^2)^2}\right.$$
$$+ \frac{(2P_\mu + q_\mu)(2P_{1\nu} - q_\nu) + (2P_\nu + q_\nu)(2P_{1\mu} - q_\mu)}{(-2P\cdot k_1 + \mu^2)(2M\nu + q^2)}$$
$$\left. + \frac{(2P_{1\mu} - q_\mu)(2P_{1\nu} - q_\nu)}{(-2P\cdot k_1 + \mu^2)^2}\right\}, \tag{17}$$

where $\mathbf{P}_1$, E_1, M, $\mathbf{k}_1$, ω_1, and μ are the momenta, energies, and masses of the proton and the pion in the final state, respectively.

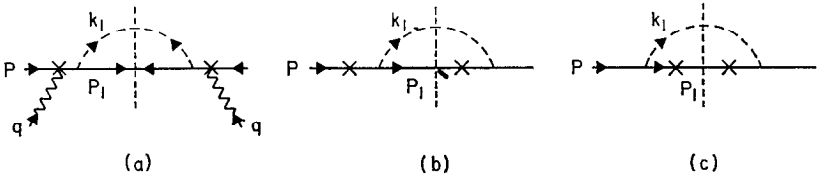

FIG. 8. Second-order Feynman diagrams for electroproduction of one pion. The crosses × indicate the electromagnetic vertex and the vertical dashed line - - - indicates that the final particles are on their mass shells.

Straightforward calculation shows

$$A = W_\mu{}^\mu = \frac{G^2}{(2\pi)^3}\frac{1}{2M}\left\{\left[\frac{q^2 + 4M\nu + 4M^2}{(q^2 + 2M\nu)^2} + \frac{2}{q^2 + 2M\nu}\right] I_0\right.$$
$$\left. + \left[\frac{2(+4M^2 - 2\mu^2 + 2M\nu)}{q^2 + 2M\nu} + 2\right] I_1 + (-q^2 + 4M^2)\, I_2\right\}; \tag{18}$$

$$B = \frac{1}{M^2}P^\mu W_{\mu\nu}P^\nu = \frac{G^2}{(2\pi)^3}\frac{1}{2M}\cdot\frac{1}{M^2}\left\{\left(\frac{+3M\nu + q^2 + 2M^2}{q^2 + 2M\nu}\right)^2 I_0\right.$$
$$\left. + \frac{2(M\nu + 2M^2 - \mu^2)(+3M\nu + 2M^2 + q^2)}{q^2 + 2M\nu} I_1 + (M\nu + 2M^2 - \mu^2)^2 I_2\right\}, \tag{19}$$

where

$$I_n = \int \frac{d^3P_1}{2E_1}\frac{d^3k_1}{2\omega_1}\,\delta^4(P + q - P_1 - k_1)\,\frac{1}{(-2P\cdot k_1 + \mu^2)^n}, \quad n = 0, 1, 2. \tag{20}$$

Elementary integrations give

$$I_0 = \frac{\pi}{2} \cdot \frac{1}{s} \sqrt{[s - (M + \mu)^2][s - (M - \mu)^2]};$$

$$I_1 = \frac{-\pi}{4M\sqrt{\nu^2 - q^2}} \times \ln \left[\frac{\left((s - q^2 + M^2)(s - M^2 + \mu^2) - 2\mu^2 s + 2M\sqrt{(-q^2 + \nu^2)[s - (M + \mu)^2][s - (M - \mu)^2]} \right)}{\left((s - q^2 + M^2)(s - M^2 + \mu^2) - 2\mu^2 s - 2M\sqrt{(-q^2 + \nu^2)[s - (M + \mu)^2][s - (M - \mu)^2]} \right)} \right]; \quad (21)$$

$$I_2 = \frac{2\pi s \sqrt{[s - (M + \mu)^2][s - (M - \mu)^2]}}{\left[[(s - q^2 + M^2)(s - M^2 + \mu^2) - 2\mu^2 s]^2 - 4M^2(-q^2 + \nu^2)[s - (M + \mu)^2][s - (M - \mu)^2] \right]};$$

where

$$s = (q + P)^2 = 2M\nu + q^2 + M^2. \quad (22)$$

In the Bjorken limit $(\lim_{BJ}) 2M\nu - q^2, -q^2, M\nu \to \infty$ with $x = (-q^2/2M\nu) < 1$ fixed, these integrals approach the limits

$$I_0 \to \frac{\pi}{2},$$

$$I_1 \to \frac{-\pi}{4M\nu} \ln \frac{2\nu}{M}, \quad (23)$$

$$I_2 \to \frac{\pi}{4M\nu} \frac{1 - x}{M^2(1 - x)^2 + \mu^2 x}.$$

By (15), (18), and (19) this leads to

$$\lim_{BJ} W_1 = 0 \left(\frac{1}{\nu} \ln \nu \right),$$

$$\lim_{BJ} \nu W_2 = \frac{G^2}{(2\pi)^3} \frac{\pi}{2} x^2(1 - x) \frac{1}{M^2(1 - x)^2 + \mu^2 x}. \quad (24)$$

It is easy to verify that this leading order of Eq. (24) is entirely due to the contribution of the third term in (17) which is due to Fig. 8c.

We now turn to the frame-dependent calculation of the same process. Here we apply the old-fashioned time-ordered perturbation theory. It is well known that a

covariant Feynman diagram decomposes into several time-ordered diagrams. For example, the Feynman diagram Fig. 8c consists of four time-ordered diagrams as represented in Fig. 9. Since time ordering is not a Lorentz invariant concept, the value of each diagram in Fig. 9 is not invariant; only their sum is.

According to the discussion above, only the four diagrams in Fig. 9 survive in the Bjorken limit. We shall therefore concentrate our attention on these four diagrams and neglect those obtained from Fig. 8a and 8b. Furthermore, W_1 vanishes in the Bjorken limit. Thus, only νW_2 will be computed in the following. Using the rules of old-fashioned perturbation theory we can verify that in frame (a) of Eq. (11) only the diagram of Fig. 9a gives a nonvanishing contribution to νW_2 in the Bjorken limit, and for this diagram we have

$$W_{\mu\nu} = \frac{G^2}{(2\pi)^3}\frac{1}{2M}\int \frac{d^3k_1}{2\omega_1}\frac{1}{2E_1'}\,\delta(q^0 + E_P - E_1' - \omega_1)\,\frac{(P_1 + P_1')_\mu\,(P_1 + P_1')_\nu}{(2E_1)^2\,(E_P - E_1 - \omega_1)^2} \tag{25}$$

where we have used the notations indicated in the figure. Let's adopt the parameterization

$$\mathbf{P}_1 = y\mathbf{P} + \mathbf{k}_\perp\,, \qquad \mathbf{k}_1 = (1-y)\,\mathbf{P} - \mathbf{k}_\perp\,, \qquad \mathbf{P}_1' = \mathbf{P}_1 + \mathbf{q}\,. \tag{26}$$

Only when $0 < y < 1$ is the integral nonvanishing and we find in the Bjorken limit

$$\begin{aligned} q^0 + E_P - E_1' - \omega_1 &= \frac{2M\nu + q^2}{4P} + \left(P + \frac{M^2}{2P}\right) \\ &\quad - \left[yP - \frac{2M\nu - q^2}{4P} + \frac{(\mathbf{q}_\perp + \mathbf{k}_\perp)^2 + M^2}{2yP}\right] \\ &\quad - \left[(1-y)\,P + \frac{k_\perp{}^2 + \mu^2}{2(1-y)\,P}\right], \\ &\cong \frac{2M\nu}{2P} - \frac{q_\perp{}^2}{2yP}\,, \\ &\cong q^0 + E_1 - E_1'; \end{aligned} \tag{27}$$

i.e., energy as well as momentum becomes conserved across the elementary electromagnetic vertex.

We can also reduce the energy denominator in (25) to

$$2E_1(E_P - E_1 - \omega_1) = -\frac{1}{1-y}\,[k_\perp{}^2 + M^2(1-y)^2 + \mu^2 y] \tag{28}$$

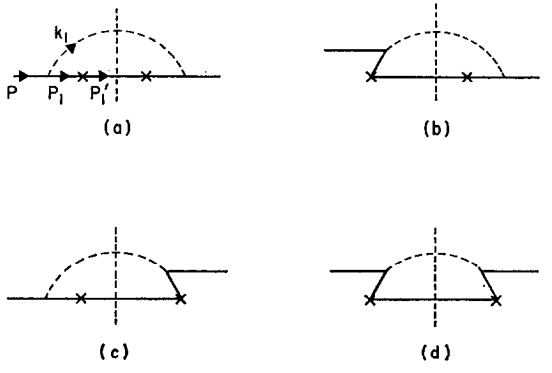

FIG. 9. Time-ordered diagrams corresponding to the single Feynman diagram of Fig. 8c.

Turning to the numerator factors we have for the large components ($\mu = 0,3$)

$$(P_1 + P_1')_\mu = 2P_{1\mu} + q_\mu = 2yP_\mu + q_\mu$$

and so leading order in frame (a)

$$W_{\mu\nu} \to \frac{1}{M^2} P_\mu P_\nu W_2$$

By identification of the coefficients of $P_\mu P_\nu$ we obtain

$$\begin{aligned} \lim_{BJ} \nu W_2 &= \frac{G^2}{(2\pi)^3} \frac{\pi}{2} \int_0^\infty dk_\perp{}^2 \, x^2(1-x) \frac{1}{[k_\perp{}^2 + M^2(1-x)^2 + \mu^2 x]^2}, \\ &= \frac{G^2}{(2\pi)^3} \frac{\pi}{2} x^2(1-x) \frac{1}{M^2(1-x)^2 + \mu^2 x}, \end{aligned} \tag{29}$$

which agrees with (24), as it should.

We now repeat the calculation in frame (b). In this frame Fig. 9b and 9c do not contribute, as can be readily verified. However, both Fig. 9a and 9d contribute generally, i.e., there occur both scattering and pair production at the external current interaction. Their contributions are, respectively

$$W_{\mu\nu}^{(a)} = \frac{G^2}{(2\pi)^3} \frac{1}{2M} \int \frac{d^3k_1}{2\omega_1} \frac{1}{2E_1'} \delta(q^0 + E_P - E_1' - \omega_1) \frac{(P_1 + P_1')_\mu (P_1 + P_1')_\nu}{(2E_1)^2 (E_P - E_1 - \omega_1)^2}$$

$$W_{\mu\nu}^{(d)} = \frac{G^2}{(2\pi)^3} \frac{1}{2M} \int \frac{d^3k_1}{2\omega_1} \frac{1}{2E_1'} \delta(q^0 + E_P - E_1' - \omega_1) \frac{(\bar{P}_1 - P_1')_\mu (\bar{P}_1 - P_1')_\nu}{(2\bar{E}_1)^2 (E_P + \bar{E}_1 - \omega_1)^2}$$

Let us use the parameterization

$$\begin{aligned} &\mathbf{P}_1 = y\mathbf{P} + \mathbf{k}_\perp, \qquad \mathbf{k}_1 = (1-y)\,\mathbf{P} - \mathbf{k}_\perp, \\ &\mathbf{P}_1' = \mathbf{P}_1 + \mathbf{q} \end{aligned} \tag{31a}$$

for Fig. 9a and

$$\begin{aligned} &\bar{\mathbf{P}}_1 = y'\mathbf{P} + \mathbf{k}_\perp', \qquad \mathbf{k}_1 = (1+y')\,\mathbf{P} + \mathbf{k}_\perp', \\ &\mathbf{P}_1' = \mathbf{q} - \bar{\mathbf{P}}_1 \end{aligned} \tag{31b}$$

for Fig. 9d. In the Bjorken limit the energy conservation equation becomes

$$\begin{aligned} q^0 + E_p - E_1' - \omega_1 = &\frac{2\nu}{M}P + \left(P + \frac{M^2}{2P}\right) \\ &- \left[\left(\frac{2\nu}{M} + y\right)P + \frac{q_\perp^2}{2(2\nu/M + y)\,P}\right] \\ &- \left[(1-y)\,P + \frac{k_\perp^2 + \mu^2}{2(1-y)\,P}\right], \\ \cong &\frac{1}{2P}\left[M^2(1-x) - \frac{k_\perp^2 + \mu^2}{1-y}\right], \end{aligned} \tag{32}$$

in terms of (31a) for Fig. 9a, and

$$q^0 + E_p - E_1' - \omega_1 \cong \frac{1}{2P}\left[M^2(1-x) - \frac{k_\perp'^2 + \mu^2}{1+y'}\right], \tag{33}$$

in terms of (31b) for Fig. 9d. For the energy denominators notice that

$$\begin{aligned} &2E_1(E_P - E_1 - \omega_1) \\ &= -\frac{1}{1-y}\,[k_\perp^2 + M^2(1-y)^2 + \mu^2 y], \\ &= -\frac{M^2(1-x)}{k_\perp^2 + \mu^2}\left\{k_\perp^2 + \frac{(k_\perp^2 + \mu^2)^2}{M^2(1-x)^2} + \mu^2\left[1 - \frac{k_\perp^2 + \mu^2}{M^2(1-x)}\right]\right\}, \\ &= -\frac{1}{1-x}\,[k_\perp^2 + M^2(1-x)^2 + \mu^2 x], \end{aligned} \tag{34}$$

where we have made use of the solution to the δ-function given by (32). Similarly, with the aid of (33) we have

$$2\bar{E}_1(E_P + \bar{E}_1 - \omega_1) = \frac{1}{1-x}\,[k_\perp'^2 + M^2(1-x)^2 + \mu^2 x]. \tag{35}$$

For the large components ($\mu, \nu = 0, 3$) the tensor structure becomes

$$W_{\mu\nu} \to \frac{1}{M^2} P_\mu P_\nu \left(\frac{M\nu}{q^2}\right)^2 \left(\frac{2\nu}{M}\right)^2 W_2 \tag{36}$$

in frame (b). Collecting the results (32), (33), (34), (35), and (36) we obtain finally

$$\begin{aligned} \nu W_2 = & \frac{G^2}{(2\pi)^3} \frac{\pi}{2} \int_0^\infty dk_\perp{}^2 \int_0^1 dy\, \delta \left[1 - y - \frac{k_\perp{}^2 + \mu^2}{M^2(1-x)}\right] \\ & \times \frac{x^2(1-x)}{[k^2 + M^2(1-x)^2 + \mu^2 x]^2} \\ & + \frac{G^2}{(2\pi)^3} \frac{\pi}{2} \int_0^\infty dk'^2_\perp \int_1^\infty dy'\, \delta \left[1 + y' - \frac{k'^2_\perp + \mu^2}{M^2(1-x)}\right] \\ & \times \frac{x^2(1-x)}{[k'^2_\perp + M^2(1-x)^2 + \mu^2 x]^2} \\ = & \frac{G^2}{(2\pi)^3} \frac{\pi}{2} \int_0^\infty dk_\perp{}^2 \frac{x^2(1-x)}{[k_\perp{}^2 + M^2(1-x)^2 + \mu^2 x]^2} \\ = & \frac{G^2}{(2\pi)^3} \frac{\pi}{2} x^2(1-x) \frac{1}{M^2(1-x)^2 + \mu^2 x}, \end{aligned} \tag{37}$$

which again agrees with (24), as it should. It is interesting to note that if $\mu^2/M^2 \geqslant 1$ then (32) can never vanish and the scattering diagram (Fig. 9a) will not contribute in this frame (b).

This elementary example of comparing the three methods of computing the same amplitude reveals the following. The first calculation does not tell whether scattering or photon dissociation is more important since the covariant perturbation method mixes together all possible time orderings in one diagram. In the infinite momentum frame of the proton in which the virtual photon has almost zero energy and longitudinal momentum, the calculation shows that only the scattering diagram contributes. Furthermore, in this frame energy as well as momentum is conserved across the bare electromagnetic vertex, i.e., the impulse approximation is valid. This leads to a simple physical picture that the proton first dissociates into its constituents following which an individual constituent is suddenly scattered by the very virtual photon. The ratio $-q^2/2M\nu$ measures the longitudinal momentum of the constituent scattered by the photon. In fact this picture persists for higher order diagrams of increasing complexity [5]. This is the parton model picture. However, we emphasize that such a picture is valid only in special infinite momentum frames of the proton. The infinite momentum center-of-mass frame for deep inelastic electron scattering is one such frame.

On the other hand, the physical picture is more complicated in a frame in which both q^0 and q_3 are proportional to $P(\nu/M) \gg P$ as in (11b). For the lowest order

diagrams, if $\mu^2/M^2 < 1$ both scattering and photon dissociation enter into play. If $\mu^2/M^2 > 1$, only photon dissociation need be cobsidered. It is disturbing that the mass ratios should enter the consideration in view of more complicated final states to be included. Furthermore, *the impulse approximation fails* and no simple interpretation can be given to the ratio $-q^2/2Mv$. As higher order diagrams are considered one can expect to find that both scattering and photon dissociation will play important and complicated roles in the deep inelastic electron proton scattering in this frame.

The parton model picture is obtained only by a proper choice of the coordinate system so that the photon dissociation diagrams can be *entirely* eliminated—they are not ignored but simply they are unimportant—in the Bjorken limit. This is possible since the relative importance of individual time-ordered diagrams is frame dependent and as a result the parton model picture is not a relativistically invariant concept. The fact that the same physical process assumes different appearances in different coordinate systems, simple in some but complicated in others, is an important lesson to learn, particularly so in the description of hadron–hadron collisions as recently emphasized by Feynman [1], and Benecke, Chou, Yang and Yen [9].

IV. Role of "Wee" Partons

The formal derivation of the parton model from (14) for the structure functions in the Bjorken limit leads to the expression

$$\lim_{\mathrm{BJ}} W_{\mu\nu} = 4\pi^2 \frac{E_P}{M} \int (dx)\, e^{iqx} \langle UP \mid j_\mu(x)\, j_\nu(0) \mid UP \rangle, \tag{38}$$

where $j_\mu(x) \equiv U(t)\, J_\mu(x)\, U^{-1}(t)$ is the undressed or bare current and

$$U \equiv U(0) = \left[\exp\left(-i \int_{-\infty}^{0} H_1(\tau)\, d\tau\right)\right]_+$$

is the U-matrix propagating the asymptotic state of a single physical proton, $\mid P\rangle$, up to time $t = 0$. Equation (38) is valid in reference frames of type (a) of Eq. (11). To derive this result the essential step is the approximation of overall energy conservation by

$$q^0 + E_P - E_n \approx q^0 + E_{uP} - E_{un}\,, \tag{39}$$

where E_{uP} and E_{un} are, respectively, the energies of the components appearing in the expansions of $\mid UP\rangle$ and $\mid Un\rangle$; viz

$$UP\rangle = \sqrt{Z_2}\,\{\mid P\rangle + \sum_{n \neq P} \frac{\langle n \mid H_1 \mid P\rangle \mid n\rangle}{E_P - E_n + i\epsilon} + \cdots . \tag{40}$$

Equation (39) is an impulse approximation, since it replaces the overall energy conservation for the interaction by energy conservation across the bare electromagnetic vertex. It is the necessary approximation for establishing scaling in the Bjorken limit. We have studied the validity of the approximation (39) and derived (38) in our earlier papers [5].

Here we analyze the role of the "wee" partons of Feynman [1] and in particular show that they do not affect the validity of the scaling arguments. In the infinite momentum frame (11a) the direction along the initial nucleon with momentum $\mathbf{P}$ and the direction of the scattered constituent's momentum $x\mathbf{P} + \mathbf{q}$ define two distinct directions for all the particles involved, virtual and real, to follow. Generally a particle will have a momentum along the direction of $x\mathbf{P} + \mathbf{q}$ if it is created by the scattered constituent; otherwise, it will have a momentum along the direction of $\mathbf{P}$. These two groups of particles will be called (B) and (A), respectively, as illustrated in Fig. 10.

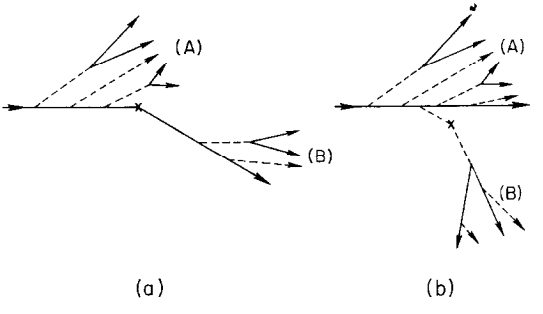

FIG. 10. Diagrams illustrating pions and nucleons moving in well-separated and well-identified groups along the directions $\mathbf{P}$ and $x\mathbf{P} + \mathbf{q}$.

A particle with a finite fraction of longitudinal momentum will belong either to group (A) or group (B) but not to both, since it has a clear sense of direction. Consequently it cannot be exchanged between the two groups which are separated by an asymptotically large transverse momentum $\mathbf{q}$. However, a very special group of particles with momenta in an extremely small kinematic region do not have a well-defined sense of direction and therefore can be associated with both of the two groups (A) and (B) without introducing a large transverse momentum mismatch as we discussed in Section II. These are the "wee" partons which introduce interactions and interferences between particles in group (A) and those in group (B). They also give rise to the dominant contributions to high energy hadron–hadron interactions as we described earlier according to the Feynman theory [1]. The "wee" partons have momenta of the following form

$$\mathbf{P}_w = y\mathbf{P} + \mathbf{k}_\perp , \tag{41}$$

where

$$yq \sim m, \qquad k_\perp \leqslant m'$$

and m and m' are typical masses assumed no larger than ≈ 1 GeV. $\mathbf{P}_w$ is closely parallel to the direction of $\mathbf{P}$ in the infinite momentum frame. However (41) can also be rewritten as

$$\mathbf{P}_w = \frac{y}{x}(x\mathbf{P} + \mathbf{q}) + \mathbf{k}_\perp - \frac{1}{x}(y\mathbf{q}) \tag{42}$$

which is also parallel to $x\mathbf{P} + \mathbf{q}$, the direction of the scattered constituent, since $\mathbf{k}_\perp - 1/x\,(y\mathbf{q})$ is finite [10] as a result of the restriction $yq \sim m$. Since their phase space diminishes to zero as $q^2 \to \infty$, it may be argued that these "wee" partons should not play any role in the Bjorken limit. Indeed this is the case order by order in the perturbation expansion for the quantum field theory model (the γ_5 theory with a $k_\perp$ cutoff of the hadronic interactions) studied in our earlier papers [5].

On the other hand, Feynman [1] argued that "wee" partons do play an essential role. As we described earlier they account for a nonvanishing total cross section in hadron–hadron collisions at very high energies and emerge as pionization products. Therefore we must understand their apparent absence from our field theory model as we applied it in the Bjorken limit for deriving scaling behavior and the parton model. The recent work of Chang and Yan [11] offers an explanation and a basis for understanding here. They work with a ϕ^3 model for calculational ease, the point being that no cutoff is required in this superrenormalizable model to suppress the high momentum components. Chang and Yan show with this model that the wee region is promoted to its prominant and essential role if the leading contributions to *all* orders in the perturbation expansion are summed up, order by order. Then if the coupling is sufficiently strong the individual contributions, though small and vanishing as $s \to \infty$, add up to give the dominant contribution to the limiting behavior. The series obtained in this work sums to

$$\frac{1}{s}\sum_{n=0} \frac{G^n \ln s}{n!} = s^{G-1} > 0 \qquad \text{as} \quad s \to \infty \quad \text{if} \quad G \geqslant 1. \tag{43}$$

We interpret this result to mean that a procedure of working to finite orders in a perturbation expansion, even with high momentum components suppressed by a cutoff as we have done, is inadequate to represent the "wee" region correctly. In fact summing to all orders the leading contribution, term by term, in the region of high ω or small x ("soft partons") was found to lead to just such an exponentiation as (43) in our earlier [5] studies of νW_2.

What must we then do? First of all we will show that the derivation of the impulse approximation and hence of the scaling behavior in the Bjorken limit, which is the central result, is unaffected by the "wee" partons. We can do this on

grounds of kinematics, without reference to a specific model by verifying that the "wee" partons do not affect the energy argument in (39). A "wee" parton can appear in (14) in three different ways: (1) it is in the expansion of UP in (40) and is absorbed by group (B) as represented by Fig. 11a; (2) it is exchanged between group (A) and group (B), as represented by Fig. 11b; (3) it appears as a real particle in the final states as represented by Fig. 11c. We now consider each of these three cases separately, assuming there is only one "wee" parton in each case. Generalization to more complicated situations is obvious.

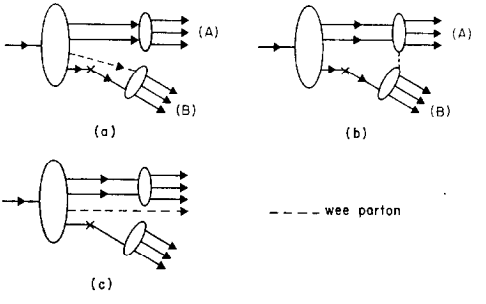

FIG. 11. Examples which show how the postulated existence of wee partons affects the picture shown in Fig. 10. The dashed line represents a wee parton or a system of wee partons.

(1) The effective squared invariant mass M^2 of a component of $|\, UP\rangle$ is

$$M^2 = \sum_i \frac{k_{i\perp}^2 + m_i^2}{x_i}, \tag{44}$$

where $x_i, k_{i\perp}, m_i$ are the fraction of longitudinal momentum, the transverse momentum, and the mass of the i-th constituent making up the particular component of $|\, UP\rangle$. If one of the particles in the above sum is wee, then as in (41) its $x_i = y \approx m/q$ and its contribution to (44) is

$$\frac{k_{i\perp}^2 + m_i^2}{x_i} \approx 0(qm), \qquad x_i \sim m/q;$$

which is smaller by order $m/\sqrt{Q^2}$ or $\sqrt{m/\nu}$ in comparison with $(2M\nu - q^2)$ which appears in q^0 of (39). Even though the invariant mass is not finite, it is smaller than the leading term by $M/\sqrt{Q^2}$. Furthermore this statement is true even if the multiplicity of "wee" constituents increases in the manner conjectured by Feynman [1] to lead to constant total cross sections for hadronic processes as we discussed in Section II, i.e., as dx/x which by (41) leads to

$$\int \frac{dx}{x} \sim \ln q/m. \tag{45}$$

The same is true for the squared invariant mass of the scattered constituent plus the wee parton in the component of $U \mid n\rangle$. Thus we still can ignore the energy differences between the states $\mid P\rangle$ and $\mid UP\rangle$, $\mid n\rangle$ and $U \mid n\rangle$. The impulse approximation is therefore valid.

(2) Again the corrections are of order $q = \sqrt{Q^2}$. To see this consider the diagram Fig. 12. The single lines P_1, P_1', P_2'' may represent groups of particles. We introduce the parameterizations (the particle with momentum k is wee)

$$\mathbf{P}_1 = (1 - x)\,\mathbf{P} - \mathbf{k}_\perp, \qquad \mathbf{k} = y\mathbf{P} + \mathbf{k}_\perp' \ (y \sim m/q),$$
$$\mathbf{P}_2 = x\mathbf{P} + \mathbf{k}_\perp,$$
$$\mathbf{P}_2' = x\mathbf{P} + \mathbf{q}_3 + (\mathbf{k}_\perp + \mathbf{q}_\perp),$$
$$\mathbf{P}_2'' = [x - y]\,\mathbf{P} + \mathbf{q}_3 + (\mathbf{k}_\perp + \mathbf{q}_\perp - \mathbf{k}_\perp'),$$
$$\mathbf{P}_1' = (1 - x + y)\,\mathbf{P} - (\mathbf{k}_\perp - \mathbf{k}_\perp').$$

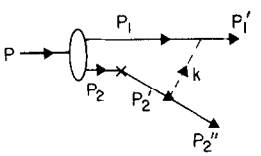

FIG. 12. Example of a final state interaction between the two groups of particles in (A) and (B) of Fig. 10 introduced by exchange of wee partons.

The energy difference between the states $\mid n\rangle$ and $U \mid n\rangle$ is computed directly as

$$\begin{aligned}
&E_1' + E_2'' - E_1 - E_2' \\
&\quad = \left[(1 - x + y)\,P + \frac{(\mathbf{k}_\perp - \mathbf{k}_\perp')^2 + M_1^2}{2(1 - x + y)\,P}\right] \\
&\qquad + \left[(x - y)\,P + q_3 + \frac{(\mathbf{k}_\perp + \mathbf{q}_\perp - \mathbf{k}_\perp')^2 + M_2^2}{2(x - y)\,P}\right] \\
&\qquad - \left[(1 - x)\,P + \frac{k_\perp^2 + M_1^2}{2(1 - x)\,P}\right] - \left[xP + q_3 + \frac{(\mathbf{k}_\perp + \mathbf{q}_\perp)^2 + M_2^2}{2xP}\right], \\
&\quad = \frac{1}{2P}\left\{\frac{(\mathbf{k}_\perp + \mathbf{q}_\perp - \mathbf{k}_\perp')^2 + M_2^2}{x - y} - \frac{(\mathbf{k}_\perp + \mathbf{q}_\perp)^2 + M_2^2}{x}\right. \\
&\qquad \left. + \frac{(\mathbf{k}_\perp - \mathbf{k}_\perp')^2 + M_1^2}{1 - x + y} - \frac{k_\perp^2 + M_1^2}{1 - x}\right\}, \\
&\quad = 0(q/P).
\end{aligned} \tag{46}$$

The leading terms proportional to $q_\perp^2$ cancel as a result of the restriction $y \sim M/q$. Thus the difference is only of order q/P which can be neglected in comparison with q^0.

(3) The arguments are similar to case (1) and therefore it will not be discussed in detail.

From the discussion above we have seen that the postulated existence of "wee" partons does not invalidate the impulse approximation (38) so long as their spectrum is not more singular than the dx/x indicated in (45). Consequently the parton model picture holds under these circumstances. Furthermore, by computing the laboratory energy of a final particle, $k_i = (1/M)\, P \cdot P_i$, in the infinite momentum frame (11a), it is straightforward to show that in the Bjorken limit the final particles are divided into three groups:

(a) the nonwee particles from group (A) of Fig. 10 have finite energies;

(b) the wee particles have energies proportional to $\sqrt{M\nu}$;

(c) the nonwee particles in group (B) have energies proportional to ν.

In addition to the deep inelastic electron (or neutrino as well as antineutrino) scattering, the impulse approximation also applies to electron–positron pair annihilation $e^+ + e^- \to H +$ "anything" in the deep inelastic region of high energy, or large incident pair mass squared, q^2, and large invariant energy transfer to the detected hadron $\nu \equiv (1/M)\, q \cdot P$. In an infinite momentum frame of the detected hadron, this process can be described [5] as the creation of an essentially free parton–antiparton pair and its subsequent decay into final states. It can also be studied in a similar fashion following the path given above. In particular the wee partons will not alter the predictions of scaling that we have derived in [5, Paper III]. The specific relation between the scattering and annihilation cross sections was based on an analysis with finite order perturbation theory which was used to derive the result that the structure functions for annihilation were continuations of those for scattering from the region $\omega > 1$ to $\omega < 1$. Whether this identification will be altered by the sum to all orders of the "wee" parton contributions is an open problem.

V. Massive Lepton Pair Production in Hadron–Hadron Collisions at Very High Energies

If we want to satisfy the kinematical constraints allowing application of the impulse approximation in hadron–hadron interactions we need look for interactions at high energies s which absorb or produce a lepton system of huge mass Q^2

such that the ratio Q^2/s is finite as we discussed in Section II. We shall discuss in detail here an observable process meeting this requirement [2], viz.,

$$p + p \to (\mu^+\mu^-) + \cdots .$$

Our remarks apply equally to any colliding pair such as (pp), $(\bar{p}p)$, (πp), (Kp), (γp) and to final leptons $(\mu^+\mu^-)$, $(e\bar{e})$, $(\mu\nu)$, and $(e\nu)$.

For finite Q^2/s one has the relation [see (10)]

$$Q^2 \cong x_1 x_2 s; \qquad 0 < x_{1,2} < 1, \tag{47}$$

where $x_{1,2}$ are the fractions of the longitudinal momenta of their respective hadrons carried by the annihilating parton–antiparton pair as illustrated in Fig. 6. Here we are dealing with hard partons and with the same region of momenta as probed by deep inelastic electron scattering experiments which measure the parton distribution $0 < x = Q^2/2M\nu < 1$. In this process we are measuring over a range of x values for antipartons as well as partons as constrained by (47) for fixed Q^2/s.

Following standard calculational steps we obtain the general expression for the cross section to form a lepton pair of mass Q^2

$$\frac{d\sigma}{dQ^2} = \left(\frac{4\pi\alpha^2}{3Q^2}\right)\sqrt{1 - \frac{4m^2}{Q^2}}\left(1 + \frac{2m^2}{Q^2}\right) \times \frac{1}{\sqrt{[s - (M_1 + M_2)^2][s - (M_1 - M_2)^2]}}\, W(Q^2, s) \tag{48}$$

where a spin average is understood and

$$\begin{aligned} W(Q^2, s) &\equiv -16\pi^2 E_1 E_2 \int (dq)\, \delta(q^2 - Q^2) \int (dx)\, e^{-iqx} \\ &\quad \times \langle P_1 P_2^{(in)} \mid J_\mu(x)\, J^\mu(0) \mid P_2 P_1^{(in)} \rangle \\ &= -16\pi^2 E_1 E_2 \int (dq)\, \delta(q^2 - Q^2) \sum_n (2\pi)^4\, \delta^4(P_1 + P_2 - q - P_n) \\ &\quad \times \langle P_1 P_2^{(in)} \mid J_\mu \mid n \rangle \langle n \mid J^\mu \mid P_2 P_1^{(in)} \rangle . \end{aligned} \tag{49}$$

In (49) E_1, P_1, M_1 and E_2, P_2, M_2 are the energies, momenta, and masses of the two initial hadrons; m is the muon mass: and Σ is a sum over all unobserved hadron states. The integral over pair momenta, d^4q, extends over the entire mass hyperboloid $q^2 = Q^2$ in the high energy limit. Restrictions on the phase space integral can be included to match experimental conditions and will be discussed later for comparison with Ref. [6].

To simplify (49) in the limit $s \to \infty$ with Q^2/s fixed, we may proceed either in the CM system of the two initial hadrons or a true infinite momentum frame defined earlier by (8). The final result, as required, is independent of the choice between the two types of coordinate systems.

Since we will imitate the steps in our preceding analysis of deep inelastic processes [5] we work in a true infinite momentum frame as introduced in Section II by boosting from the collision center-of-mass frame by a velocity $\beta/\sqrt{1-\beta^2} = 2P/\sqrt{s}$ in a direction orthogonal to the collision axis. The four-vector momenta of the two incident colliding hadrons are then as in (8) for $s \gg M^2$

$$P_1^\mu = \left(P + \frac{s}{8P}, 0, P, \frac{1}{2}\sqrt{s}\right),$$
$$P_2^\mu = \left(P + \frac{s}{8P}, 0, P, -\frac{1}{2}\sqrt{s}\right). \tag{50}$$

We can now let $P \to \infty$ for large but finite s: $P \gg \sqrt{s} \gg M$. The energy in the collision is represented by a transverse momentum mismatch of the two colliding hadrons. For a parton, or a baryon or meson quantum in our field theory model, to be exchanged between them without introducing an asymptotically large momentum transverse to either of the two hadron lines, the parton momentum is restricted to a fraction $\sim M/\sqrt{s}$ along the $\mathbf{P}$ axis and to a finite value $\sim M$ orthogonal to it. This constraint corresponds to the "wee" parton condition in the center-of-mass frame of the colliding hadrons. In the $P \to \infty$ frame (50) this constraint satisfies the condition of finite transverse momentum imposed on our field theory model.

In this frame [2] we can repeat steps developed in earlier work of undressing the current operator by the U matrix: $J_\mu(0) = U^{-1} j_\mu(0)\, U$ where $j_\mu(0)$ is the current operator expressed in terms of free fields. Furthermore the energy differences between the eigenstate $|\, P_1 P_2^{(in)}\rangle$ and the components of $U(P_1P_2)^{in}\rangle$ can be ignored in the limit $s \to \infty$ for Q^2/s finite; the same is true for $|\, n\rangle$ and $U\,|\, n\rangle$. This is so because the invariant mass of the individual system of particles moving along $\mathbf{P}_1$ and $\mathbf{P}_2$ respectively in (50), or to the right and left in the center-of-mass frame, is negligible compared with the invariant mass $\frac{1}{2}\sqrt{s}$ appearing in (50) as a result of the transverse momentum cutoff imposed. In other words the impulse approximation is good and energy as well as momentum is conserved across the electromagnetic current vertex in (49). This leads to the simplification in the $\lim_{BJ}$ for $P \to \infty$; $s \gg M^2$; Q^2/s finite to

$$\lim_{BJ} W = -16\pi^2 E_1 E_2 \int (dq)\, \delta(q^2 - Q^2) \int (dx)$$
$$\times\, e^{-iqx} \langle U(P_1P_2)^{in} \,|\, j_\mu(x)\, j^\mu(0) \,|\, U(P_2P_1)^{in}\rangle. \tag{51}$$

A remark about the result (51) is in order because in our earlier work it was only the "good" components of the current (i.e., $\mu = 0$ and 3) that were explicitly studied and for which "undressing" was derived. Here we have to deal with a scalar product involving all four components. The "bad" components transverse to the infinite momentum direction give rise to the following complication. In the true infinite momentum frame (50), for a current component transverse to $\mathbf{P}$ the electromagnetic vertex is of order $\mathbf{P}$ when the colliding parton and antiparton are of spin 1/2 and have longitudinal momenta opposite in direction relative to $\mathbf{P}$ as shown by

$$\bar{u}(x_1\mathbf{P} + \mathbf{k}_{1\perp}\,;\, s_1)\,\gamma_\perp v(-x_2\mathbf{P} - \mathbf{k}_{2\perp}\,;\, s_2) = \frac{P}{M}\sqrt{x_1x_2}\,\chi^*(s_1)\,\sigma_\perp\chi(-s_2) + 0(1), \quad (52)$$

where χ is a two-component Pauli spinor. In such a case, however, the factor P in (52) is used in conjunction with another factor of P coming from a strong vertex which also behaves like a bad current and is very large, $\sim P$, when producing, annihilating, or scattering fermions with opposite sense of motion along $\mathbf{P}$. These two factors of P compensate the $1/P^2$ factor introduced by the bad energy denominator associated with an intermediate state involving particles of opposite longitudinal momenta. Thus, effectively, the electromagnetic vertex is of order unity. On the other hand, however, when all the particles move along the direction of the infinite momentum, the electromagnetic vertex of a transverse component of the current is of order $\sqrt{s}$, introduced by the large transverse momentum mismatch of the colliding spin 1/2 parton–antiparton pair. And there are no powers of P to cancel [12]. Consequently as $s \to \infty$ the contribution is negligible from an electromagnetic vertex with the annihilating parton–antiparton pair moving in opposite directions relative to $\mathbf{P}$. Thus, the result (51) is valid in frame (50) for all four components of the current. The arguments given here are similar to those given in [5, Paper IV] in connection with neutrino scattering in which the use of transverse components of the current is also required. The key in deriving (51) as shown by our earlier work is that all particles be moving along the $\mathbf{P} \to \infty$ direction at the instant of the current interaction, and the above argument verifies it in the high energy limit.

Turning to the situation in the CM system, we expect each member of the annihilating pair to retain the direction of its original hadron. For such a case, i.e., the colliding parton and antiparton moving in opposite directions, it is interesting to notice that the transverse components of the currents for spin 1/2 particles are the "good currents" and in this problem their vertices are of order $P = 1/2\sqrt{s}$ [see (52)]. When both of the pair move along the same direction, the corresponding vertices are of order unity. The reverse is true for the third and time components of the current. However, the unnatural possibility for the time and third components (with both particles moving along the same direction) can be

dismissed by a discussion similar to the previous one given in the true infinite momentum frame (50). Thus, again the result (51) is also valid for all components of the current in the CM system.

Although the above discussion shows that the contribution of individual current components is very different in the two frames, the CM system and (50), we will now show that the final result is invariant as it should be. Proceeding in analogy with [5, Paper II, Eqs. (72)–(78)] we find for the annihilation of a boson pair

$$\begin{aligned}(-)\int (dq)\,\delta(q^2 - Q^2)\int (dx)\,e^{-iqx}\langle k_1 k_2 \mid j^\mu(x)\, j_\mu(0) \mid k_2 k_1\rangle \\ = (2\pi)^4\,\delta[Q^2 - (k_1 + k_2)^2]\,\frac{-\lambda^2}{(2\pi)^6\,(2\omega_1)(2\omega_2)}\,(k_1 - k_2)_\mu\,(k_1 - k_2)^\mu, \\ = \frac{\lambda^2}{16\pi^2 E_1 E_2}\,\delta(x_1 x_2 - \tau); \qquad \tau \equiv Q^2/s < 1,\end{aligned} \tag{53}$$

where λ^2 is the square of the charge of an individual parton and we have used the high energy approximation for the dominant large components of the momenta $k_1^\mu = x_1 P_1^\mu$, $k_2^\mu = x_2 P_2^\mu$. For a fermion pair annihilation, we find

$$\begin{aligned}(-)\int (dq)\,\delta(q^2 - Q^2)\int (dx)\,e^{-iqx}\langle p_1 s_1\,,\, p_2 s_2 \mid j_\mu(x)\, j^\mu(0) \mid p_2 s_2',\, p_1 s_1'\rangle \\ = (2\pi)^4\,\delta[Q^2 - (p_1 + p_2)^2]\,\frac{-\lambda^2}{(2\pi)^6\,(2E_1)(2E_2)}\,4M^2 \bar{u}_1 \gamma_\mu v_2 \cdot \bar{v}_2' \gamma^\mu u_1'.\end{aligned} \tag{54}$$

To simplify this expression, observe the identity

$$\begin{aligned}\bar{u}_1 \gamma_\mu v_2 \bar{v}_2' \gamma^\mu u_1' = &-\tfrac{1}{4}[\bar{u}_1 \gamma_\mu (1 + \gamma_5)\, u_1' \bar{v}_2' \gamma^\mu (1 + \gamma_5)\, v_2 \\ &+ \bar{u}_1 \gamma_\mu (1 - \gamma_5)\, u_1' \bar{v}_2' \gamma^\mu (1 - \gamma_5)\, v_2 \\ &- 4\bar{u}_1 u_1' \bar{v}_2' v_2]\end{aligned} \tag{55}$$

which shows clearly that the helicities of the annihilating pair must be opposite and the helicities are conserved, since the last term in (55) is negligible in the high energy limit. Now (54) and (55) lead in the high energy limit to

$$\bar{u}_1 \gamma_\mu v_2 \bar{v}_2' \gamma^\mu u_1' = -\frac{1}{4}\left[\frac{2p_{1\mu}}{M} \cdot \frac{2p_2^\mu}{M}\right] \delta\sigma_1\sigma_1'\,\delta\sigma_2\sigma_2'\,\delta\sigma_1\,,\,-\sigma_2\,, \tag{56}$$

where the σ's denote the helicities. Using the high energy approximation $p_{1,2}^\mu = x_{1,2} P_{1,2}^\mu$, we obtain

$$\begin{aligned}(-)\int (dq)\,\delta(q^2 - Q^2)\int (dx)\,e^{-iqx}\langle p_1 s_1\,,\, p_2 s_2 \mid j_\mu(x)\, j^\mu(0) \mid p_2 s_2',\, p_1 s_1'\rangle \\ = \frac{\lambda^2}{16\pi^2 E_1 E_2}\,\delta(x_1 x_2 - \tau) \cdot 2\delta\sigma_1\sigma_1'\,\delta\sigma_2\sigma_2'\,\delta\sigma_1\,,\,-\sigma_2\,.\end{aligned} \tag{57}$$

After a spin average (57) gives the same result as (53). As our procedure is covariant in every step, the result (57) is valid in the infinite momentum frame (50) and in the CM system. Using (52), (53), and (57) and inserting the identity

$$1 = \int_0^1 d\left(\frac{1}{\omega_1}\right) \int_0^1 d\left(\frac{1}{\omega_2}\right) \delta\left(x_1 - \frac{1}{\omega_1}\right) \delta\left(x_2 - \frac{1}{\omega_2}\right)$$

we can bring (51) to the form

$$\lim_{\mathrm{BJ}} W(Q^2, s) = \sum_a \lambda_a{}^2 \int_0^1 d\left(\frac{1}{\omega_1}\right) \int_0^1 d\left(\frac{1}{\omega_2}\right) \delta\left(\frac{1}{\omega_1\omega_2} - \tau\right)$$
$$\times \langle U(P_1P_2)^{in} \mid \delta\left(x_{1,a} - \frac{1}{\omega_1}\right) \delta\left(x_{2,a} - \frac{1}{\omega_2}\right) \mid U(P_2P_1)^{in}\rangle, \quad (58)$$

where the summation over types of partons with charges λ_a pairs a parton of type a with its antiparton $\bar{a}$.

The right side of (58) depends on the dimensionless ratio $\tau = Q^2/s$, as explicitly indicated. It may also be a function of the total energy $s = (P_1 + P_2)^2$ via the states $U(P_1P_2)^{in}\rangle$. Such s dependence could enter into the expansion coefficients of $U(P_1P_2)^{in}\rangle$, which is the hadronic state at the instant $t = 0$ that develops under the influence of the full hadronic dynamics from a two nucleon "in"-state at $t \to -\infty$ of total energy s:

$$U(P_1P_2)^{in}\rangle = \sum_n C_n(s) \mid n\rangle$$
$$\sum_n \mid C_n(s)\mid^2 = 1. \quad (59)$$

If we assume that there exists a high energy limiting behavior to the expansion coefficients for the n particle states, i.e.,

$$\lim_{s\to\infty} C_n(s) = C_n\,, \quad (60)$$

then, in this limit, (58) will be independent of s and we can write

$$\lim_{\mathrm{BJ}} W(Q^2, s) = W(\tau). \quad (61)$$

Then from (48) we can write the differential cross section in a simple scaling form

$$\frac{d\sigma}{dQ^2} = \left(\frac{4\pi\alpha^2}{3Q^2}\right) \frac{1}{Q^2}\, \tau W(\tau), \quad (62)$$

$4\pi\alpha^2/3Q^2$ is just the total cross section for $e\bar{e}$ annihilation into point muon pairs in the relativistic limit. Thus a nontrivial scaling result of the form (62) follows from existence of the high energy limiting behavior of (60). In our field theory model [5] as described and discussed in Section IV the "wee" parton exchanges can be ignored as unimportant when we compute processes such as these with hard partons. With "wee" partons ignored, the state (59) can be factored into the "right" and "left" moving constituents associated, respectively, with P_1 and P_2 so that we can write

$$U(P_1P_2)^{in}\rangle \xrightarrow[\text{"no wees"}]{} |\, UP_1\rangle \,|\, UP_2\rangle. \tag{63}$$

Introducing (63) into (58) we see by comparison with (78), (79), and (80) of [5, Paper II] that (58) can be rewritten as

$$\begin{aligned} \mathscr{F}(\tau) &\equiv \tau \lim_{\text{BJ}} W(Q^2, s) \\ &= \sum_a (\lambda_a)^{-2} \int_1^\infty d\omega_1 \int_1^\infty d\omega_2\, \delta\left(\omega_1\omega_2 - \frac{1}{\tau}\right) F_{2a}(\omega_1)\, F'_{2\bar{a}}(\omega_2), \end{aligned} \tag{64}$$

in terms of the invariant structure functions $F_{2a}(\omega_1) = \nu W_2^{(\lambda_a)}$ introduced in the deep inelastic scattering analyses (see (78) of [5, Paper II]) for $1/\omega_1$ times the probability of finding parton of type a in the proton (or hadron (A) in Fig. 6) with a momentum fraction $x_1 = 1/\omega_1$. $F'_{2\bar{a}}(\omega_2)$ has the same significance for the corresponding antiparton distribution in hadron (B).

The differential cross section (62) now assumes the simple form in the scaling limit

$$\begin{aligned} \frac{d\sigma}{dQ^2} &= \left(\frac{4\pi\alpha^2}{3Q^2}\right)\left(\frac{1}{Q^2}\right) \mathscr{F}(\tau) \\ &= \left(\frac{4\pi\alpha^2}{3Q^2}\right)\left(\frac{1}{Q^2}\right) \int_0^1 dx_1 \int_0^1 dx_2\, \delta(x_1x_2 - \tau) \sum_a \lambda_a^{-2} F_{2a}(x_1)\, F'_{2\bar{a}}(x_2), \end{aligned} \tag{65}$$

where we have rewritten the invariant structure functions in terms of momentum fraction x. Presumably the "wee" quanta ignored in deriving (65) from a factored state (63) are needed to generate Feynman's spectrum of "wee" or infrared quanta, dx/x, for explaining real hadron cross sections as we described in Section II. As we also discussed earlier the "wee" region is prominent only when we sum their contributions to all orders, a la Chang and Yan [11], although to each finite order of calculation they are unimportant. We can verify explicitly that, order by order, the "wee" partons have no effect on our results for massive lepton pair production. To show this let us suppose that we include "wee" parton exchanges between the

two systems (A) and (B) before or after the parton–antiparton annihilation takes place in Fig. 6. Precisely because the transferred momenta are "wee", these interactions can change the kinematic relations only by a relatively negligible amount.

As a simple example consider the diagram in Fig. 13 in which the momentum k is wee and we are in the CM system. It can be easily checked that the impulse approximation is valid and that energy conservation requires (with neglect of masses and transverse momenta)

$$2P = (1 - x_1 - x)\,P + (1 - x_2 - x)\,P + \sqrt{(x_1 - x_2)^2\,P^2 + Q^2}$$

or

$$x_1 + x_2 + 2x = \sqrt{(x_1 - x_2)^2 + 4\,\frac{Q^2}{s}}\,.$$

But $x \sim 1/P$, so it can be neglected and

$$x_1 x_2 = Q^2/s.$$

These corrections therefore do not affect our arguments leading to (51) which in turn implies (58) and the general scaling (62). Therefore although the invariant function $\mathscr{F}(\tau)$ will be modified from (64) to (61) by the "wee" exchanges when fully computed to all orders, the general scaling property will not be affected. Based on this observation we would like to emphasize that although "wee" exchanges must survive at infinite energies to account for a nonvanishing total cross section of hadron–hadron collisions, they are not relevant to the massive muon pair production in proton–proton scattering considered here. We argued in Section IV that they also did not affect the Bjorken scaling behavior of deep inelastic lepton processes such as electron scattering and electron–positron annihilation. A nontrivial Bjorken scaling behavior and the validity of the impulse approximation for these processes are independent of whether or not the total cross section for hadrons vanishes at high energies.

In addition to scaling, there are a number of general features of the cross section that can be established without specific reference to the role of the "wee" partons.

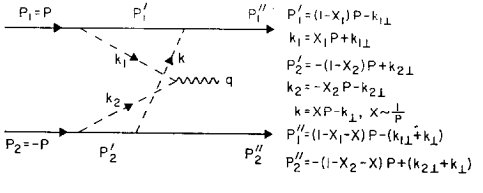

FIG. 13. Example of an initial state interaction in massive pair production in proton–proton scattering.

These include a sum rule, the angular distribution, and the polarization of the current, or massive lepton pair, emerging from the interaction:

(1) A *sum rule* can be derived from (48) and (58) in the high energy limit $s \to \infty$ by forming the weighted cross section integral

$$\int_0^1 (Q^2)^2 \frac{d\sigma}{dQ^2} \frac{d\tau}{\tau} = \int_0^s Q^2 \frac{d\sigma}{dQ^2} dQ^2 = \frac{4\pi\alpha^2}{3} \langle U(P_1P_2)^{in} \mid \sum_a \lambda_a^2 \mid U(P_1P_2)^{in} \rangle. \quad (66)$$

Equation (66) is analogous to the sum rule for the sum of the mean square charges of the partons, or constituents in the one proton state (see (78) and (81) of [5, Paper II])

$$\int_1^\infty \frac{d\omega}{\omega} (\nu W_2) = \int_0^1 \frac{dx}{x} F_2(x) = \langle UP \mid \sum_a \lambda_a^2 \mid UP \rangle, \quad (67)$$

and is subject to the same question of convergence, i.e., does the integral exist. In neither case is it experimentally clear. In terms of a factorized model with no "wee" partons we can use (65) to reduce (66) to

$$\int_0^1 (Q^2)^2 \frac{d\sigma}{dQ^2} \frac{d\tau}{\tau} = \frac{4\pi\alpha^2}{3} \sum_a \left\{ \frac{1}{\lambda_a^2} \int_0^1 F_{2a}(x) \frac{dx}{x} \int_0^1 F'_{2a}(y) \frac{dy}{y} \right\}. \quad (68)$$

Both (67) and (68) involve the same weighting of the parton momentum distribution. Higher moments can also be introduced for better convergence

$$\int_0^1 (Q^2)^2 \frac{d\sigma}{dQ^2} \tau^{n-1} d\tau = \frac{4\pi\alpha^2}{3} \sum_a \left\{ \frac{1}{\lambda_a^2} \int_0^1 F_{2a}(x) x^{n-1} dx \int_0^1 F'_{2\bar{a}}(y) y^{n-1} dy \right\}. \quad (69)$$

These relations may be of use in comparing specific parton models. Returning to (48) and (49) we can identify the general ingredient of the sum rule (66) as a spectral constraint. In (49) an integral over the entire range of masses $\int_{-\infty}^{\infty} dQ^2$ allows closure to be carried out. Experimentally however the range is confined to the time-like interval $0 < Q^2 < s$. The parton model, and in particular the prediction that it is via the parton–antiparton annihilation described in Fig. 6 and with the kinematic relation $0 < x_1x_2 = Q^2/s < 1$, ensures that the dominant contribution at high energies comes only from the time-like region $0 < Q^2 < s$ and thus permits closure in (49). We find then

$$\int_0^s dQ^2 \, W(Q^2, s) = 16\pi^2 E_1 E_2 (2\pi)^4 \langle U(P_1P_2)^{in} \mid -j_\mu(0) \, j^\mu(0) \mid U(P_1P_2)^{in} \rangle \quad (70)$$

in the parton model.

(2) The *angular distribution* of the vector $\mathbf{q} \equiv \mathbf{P}_+ + \mathbf{P}_-$, the total momentum of the muon pair, is peaked along the incident nucleon's direction in the lab system. This follows from the observation that $q \cdot P_1 = (x_1 P_1 + x_2 P_2) \cdot P_1 \cong \frac{1}{2} x_2 s$ and $q \cdot P_2 \cong \frac{1}{2} x_1 s$ are invariant, and in terms of laboratory variables we have

$$q \cdot P_2 = q_L{}^0 M_2 \,. \tag{71}$$

Denoting by θ_L the angle between $\mathbf{q}$ and $\mathbf{P}_1$ in the lab we write

$$\sin \theta_L = \frac{q_\perp}{|\,\mathbf{q}_L\,|} = \frac{q_\perp}{\sqrt{(q_L{}^0)^2 - Q^2}} \tag{72}$$

The transverse momentum cutoff that appears in our analysis limits

$$q_{\perp \max} \approx 2 \times 400 \text{ MeV} = 800 \text{ MeV}. \tag{73}$$

It follows then that

$$\theta_L \lesssim \frac{M^2}{x_1 s} \sim \frac{M^2}{Q^2} \,. \tag{74}$$

We expect to see such a strong peaking in the cross section for

$$\frac{d\sigma}{dQ^2\, dq_\perp} = \left(\frac{4\pi\alpha^2}{3Q^2}\right) \sqrt{1 - \frac{4m^2}{Q^2}} \left(1 + \frac{2m^2}{Q^2}\right) \times \frac{1}{\sqrt{[s - (M_1 + M_2)^2][s - (M_1 - M_2)^2]}}\, W_\perp(Q^2, q_\perp, s), \tag{75}$$

with

$$W_\perp(Q^2, q_\perp, s) \equiv -16\pi^2 E_1 E_2 \int dq_3\, dq_0\, \delta(q^2 - Q^2) \int (dx) \times e^{-iqx} \langle P_1 P_2^{(in)} \mid J_\mu(x)\, J^\mu(0) \mid P_2 P_1^{(in)} \rangle. \tag{76}$$

(3) In order to determine the *angular distribution of the lepton pair* emerging from the interaction we want to examine the contribution of each current component in the CM system of the collision. In this system the asymptotically large vector $\mathbf{q}$ coincides in direction, neglecting finite bounded transverse momenta of the annihilating parton and antiparton, with the collision axis of the two initial hadrons. Thus the contributions of the transverse current components correspond to the production of a transversely polarized virtual photon while the contributions of the longitudinal and time components of the current correspond to the production of a longitudinally polarized virtual photon. For this purpose we must com-

pute the contribution of each component of the current, not just the scalar product as in (55). Using (52) and the fact that

$$\bar{u}(x_1\mathbf{P} + \mathbf{k}_{1\perp}) \begin{Bmatrix} \gamma^0 \\ \gamma_3 \end{Bmatrix} v(-x_2\mathbf{P} - \mathbf{k}_{2\perp}) = 0(1), \tag{77}$$

we find that the dominant contribution for a spin 1/2 pair annihilation comes from the transverse components of the current. Moreover, explicit calculation using (52) verifies that the right side of (57) is entirely due to the sum of the two transverse components.

On the other hand, for a spin 0 pair annihilation the dominant contribution comes from the longitudinal and time components of the current, since in (53)

$$\begin{aligned}(k_{13} - k_{23})^2 - (k_1{}^0 - k_2{}^0)^2 &= (x_1 + x_2)^2 P^2 - (x_1 - x_2)^2 P^2, \\ &= x_1 x_2 s,\end{aligned} \tag{78}$$

while

$$(\mathbf{k}_{1\perp} - \mathbf{k}_{2\perp})^2 \lesssim k_{\perp \max}^2 . \tag{79}$$

This observation leads to the conclusion that if a spin 1/2 current is dominant the virtual photons produced are predominantly transversely polarized, while if a spin 0 current is dominant the virtual photons produced should be predominantly longitudinally polarized. These two cases correspond to a distribution in the center-of-mass system of the lepton pair that varies as $(1 + \cos^2 \theta)$ for spin 1/2 partons and as $\sin^2 \theta$ for spin 0 partons where θ is the angle of the lepton relative to the virtual time-like photon direction.

The data of deep inelastic electron scattering suggest that a spin 1/2 current is dominant. Accordingly this would lead us to expect that the time-like virtual photons in the μ-pair production in this deep inelastic region should be predominantly transversely polarized.

The above results can of course also be transcribed directly to the weak currents, i.e., the production of a $\mu^+\nu$ or $\mu^-\bar{\nu}$ pair by pp scattering. The correspondence with the $\mu^+\mu^-$ pair production is given by the substitution

$$\begin{aligned}\frac{4\pi\alpha}{Q^2} &\to \frac{G}{\sqrt{2}} \frac{M_W{}^2}{M_W{}^2 - Q^2}, \\ J_\mu &\to J_\mu{}^c,\end{aligned} \tag{80}$$

where G is the Fermi coupling constant, M_W the mass of the intermediate vector boson and $J_\mu{}^c$ the Cabbibo current. A factor of 2 should also be introduced into $d\sigma/dQ^2$ as the vector and axial part of the lepton current contribute equally. There is no interference between the axial and vector current if only the total momentum

vector q_μ of the pair is observed. The differential cross section for producing $\mu^-\bar{\nu}$ pairs with squared invariant mass Q^2 is

$$\frac{d\sigma}{dQ^2}(\mu^-\bar{\nu}) = \frac{G^2}{12\pi} Q^2 \left(\frac{M_W{}^2}{Q^2 - M_W{}^2}\right)^2 \times \frac{1}{\sqrt{[s - (M_1 + M_2)^2][s - (M_1 - M_2)^2]}} W'(Q^2, s), \quad (81)$$

where a spin average is understood and

$$W'(Q^2, s) = -16\pi^2 E_1 E_2 \int (dq)\, \delta(q^2 - Q^2) \int (dx) \times e^{-iq\cdot x} \left(g^{\mu\nu} - \frac{q^\mu q^\nu}{q^2}\right) \langle P_1 P_2^{(in)} \mid J_\mu^{c\dagger}(x)\, J_\nu^c(0) \mid P_2 P_1^{(in)} \rangle. \quad (82)$$

In (81) the lepton masses are neglected. In the scaling limit we have

$$\lim_{\text{BJ}} W'(Q^2, s) = W'(\tau) \quad (83)$$

and

$$\frac{d\sigma}{dQ^2}(\mu^-\bar{\nu}) = \frac{G^2}{12\pi} \left(\frac{M_W{}^2}{M_W{}^2 - Q^2}\right)^2 \tau W'(\tau). \quad (84)$$

Notice that if the vector boson does not exist—or has infinite mass so that the weak interaction is local—we take the limit $\{M_W{}^2/M_W{}^2 - Q^2)\} \to 1$. Then the differential cross section $d\sigma/dQ^2$ becomes scale invariant. It is independent of Q^2 and is a function of the ratio $\tau = Q^2/s$ only. It will be of particular interest to search for a deviation from such a scaling law for the weak currents if scaling is verified for the electromagnetic pair production. If such a deviation is observed as an enhancement at high Q^2 and can be fit to a form $[M_W{}^2/(M_W{}^2 - Q^2)]^2$, we can interpret it in terms of a finite mass for the vector boson of the weak interactions.

With the neglect of "wee" parton contributions (58) reduces to (64) and the cross section can be expressed as a product of structure functions for the parton and antiparton distributions in one-body states. These distributions are integrated over all momentum fractions x_1 and x_2 consistent with the kinematic constraint $x_1 x_2 = Q^2/s = \tau$. Deep inelastic electron scattering measures the sum of the parton and antiparton contributions as a function of $0 < x \equiv Q^2/2M\nu < 1$. Here however we require the product of these contributions. To help unravel these individual terms it would also be of great interest to study $\bar{p}p$ as well as pp scattering. Moreover the full range of possibilities including πp, kp, γp will be of great interest to study in order to compare their spectra, as well as to measure their effective charges λ^2. [*Note added in proof*: A study of the γp-process has been completed by R. L. Jaffe to appear in *Phys. Rev.*]

These comparisons are dependent however on the assumption that wee partons can be ignored. There is no small expansion parameter in terms of which to measure the quality of such an approximation. The problem presented by the "wee" partons is illustrated in Fig. 14. What we show here is elastic exchange of a single "wee" parton between the two colliding protons. Since the wee exchanges involve large energy denominators as we recall from (1) we may view them as occurring instantaneously on the longer time scale of the hard parton states. With the momentum labels as drawn this exchange has introduced a momentum dependence via an energy denominator

$$\frac{1}{E_{x_1\mathbf{P}+\mathbf{k}_{1\perp}} - E_{x_1\mathbf{P}-\alpha i_p+\mathbf{k}_{1\perp}-\mathbf{q}_\perp} - \omega_{\alpha i_p+\mathbf{q}_\perp}} \approx \frac{1}{\alpha - \sqrt{\alpha^2 + {q_\perp}^2 + \mu^2}}, \tag{85}$$

and has coupled the transverse momentum structure of the two-proton states. Factoring as in (63) is hence impossible and we can no longer derive the product form of (65). As emphasized earlier the scaling dependence is unaffected. In the limit of purely forward scattering by the wee exchanges this problem can be avoided since no change occurs in the transverse momenta. Moreover the change of longitudinal momenta is of order $1/P$ and negligible. However we know that the wee exchanges must do more than simply forward scatter at 0^0. Experimentally the high energy cross sections have diffraction peaks that typically are of 350–400 MeV/c width in transverse momentum and this, being comparable to the transverse momenta appearing in our parton distribution, cannot in general be neglected. Our formal theoretical methods are not adequate for making a more detailed study of the role of these wee exchanges and their effect on the τ dependence of $\mathscr{F}(\tau)$. If we simply ignore them we can make some qualitative observations from the comparison of (65) with the preliminary data of Ref. [6].

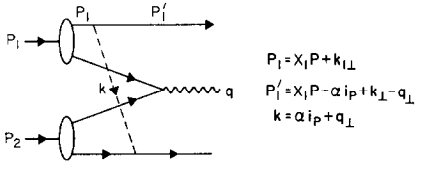

FIG. 14. Example to illustrate how the initial state interaction due to wee exchange affects the structure function for massive pair production.

The data to which we want to compare (65) was obtained by taking a limited cut of the events leading to a given lepton pair mass of Q^2. Only those events were detected for high energy protons incident on a uranium nucleus leading to muon pairs of total momentum $q \geqslant 12$ GeV/c and emerging with $q_\perp/q \leqslant 1/16$ in the

laboratory system. Therefore these actual experimental resolution functions must be introduced before a detailed comparison can be made. The angular constraint includes all transverse momenta up to at least $q_\perp = 1/16(12\ \mathrm{GeV}/c) = 750\ \mathrm{MeV}/c$. This value is sufficiently close to our actual transverse momentum cutoff in (73) that for purpose of comparison we include all solid angles in (65). However a longitudinal momentum cutoff corresponding to $q_{\min} = 12\ \mathrm{GeV}/c$ must be introduced as we do in the following way. Denoting the laboratory momentum of the target nucleon by

$$P_2{}^\mu = (M_2\,, 0) \text{ and the pair by } q^\mu = (q_{\mathrm{L}}{}^0,\ q_{\mathrm{L}}) \tag{86}$$

we can write the magnitude of the pair momentum in the laboratory frame as

$$q_{\mathrm{L}} = \sqrt{(q \cdot P_2)^2/M_2{}^2 - Q^2} \equiv \sqrt{q_{\mathrm{L}}^{02} - Q^2}. \tag{87}$$

An invariant expression for $q_{\mathrm{L}}{}^0$ in terms of the fraction of momenta on the colliding parton pair is given by

$$M_2 q_{\mathrm{L}}{}^0 = q \cdot P_2 = P_2 \cdot (x_1 P_1 + x_2 P_2) \approx \tfrac{1}{2} x_1 s. \tag{88}$$

We can also write, as we already have a number of times,

$$Q^2 = x_1 x_2 s.$$

Collecting we have in the kinematic region of interest

$$q_{\mathrm{L}} = \sqrt{\left(\frac{s x_1}{2M_2}\right)^2 - s x_1 x_2} \approx \frac{s}{2M_2}\, x_1\,. \tag{89}$$

The content of (89) is that the asymptotically large momentum of the lepton pair is given simply by the incident nucleon momentum, $s/2M_2$ in the laboratory system, multiplied by x_1, the fraction of that momentum carried by the annihilating parton. In this limit the momentum components in the target state (at rest) are negligible. The experimental constraint that $q_{\mathrm{L}} > q_{\mathrm{L\,min}} = 12\ \mathrm{GeV}/c$ now can be expressed as a step function to be inserted directly into (65):

$$\begin{aligned}\left(\frac{d\sigma}{dQ^2}\right)_E &= \left(\frac{4\pi\alpha^2}{3Q^2}\right)\left(\frac{1}{Q^2}\right)\int_0^1 dx_1 \int_0^1 dx_2 \\ &\quad \times \frac{1}{2}\left[\theta\left(x_2 - \frac{2M_1 q_{\mathrm{L\,min}}}{s}\right) + \theta\left(x_1 - \frac{2M_2 q_{\mathrm{L\,min}}}{s}\right)\right] \\ &\quad \times \delta(x_1 x_2 - \tau) \sum_a \frac{1}{\lambda_a{}^2} F_{2a}(x_1)\, F'_{2\bar{a}}(x_2), \\ &\equiv \left(\frac{4\pi\alpha^2}{3Q^2}\right)\frac{1}{Q^2}\,\mathscr{F}_E(\tau).\end{aligned} \tag{90}$$

In writing (90) we have symmetrized the expression in terms of parton and antiparton. The sum is to be taken over different types of antipartons as well as partons. The observed rapid decrease of the inelastic structure functions $F_2(x) = \nu W_2$ as $x \to 1$ leads in (65) and (90) to a prediction of a very rapid falloff in $\mathscr{F}_E(\tau)$ with increasing Q^2, or τ. If we assume that the parton and antiparton have identical momentum distributions in the proton, and this is common for all parton types λ, we can compute $d\sigma/dQ^2$ directly from measured $F_2(x)$, finding a very rapid falloff in the cross section as shown in Fig. 15, even though the model consists of point-like constituents. For comparison a dotted curve is drawn in Fig. 15 to show the effect of the experimental resolution in reducing the cross section below the full value in (65). The slope of the theoretical curve fits the preliminary experimental findings in the range of Q^2 from $Q^2 = 2(\text{GeV}/c)^2$ to $Q^2 = 10\,(\text{GeV}/c)^2$. However there is an apparent bump in the observed spectrum that exceeds our calculated curve by a factor of 2–3 in the interval of $Q^2 = 10$–$20\,(\text{GeV}/c)^2$.

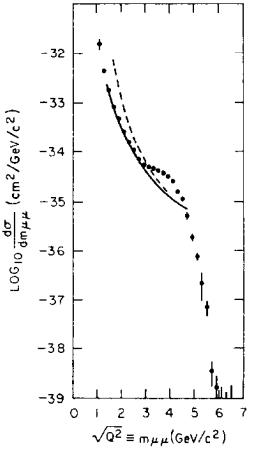

FIG. 15. $d\sigma/d\sqrt{Q^2}$ computed from Eq. (90) assuming identical parton and antiparton momentum distributions. The normalization is fitted to the curve. The solid curve includes the effect of the experimental resolution $q_L > 12$ GeV. The dashed curve includes all phase space.

We will not speculate here on the possible significance of such a bump [13]. Recall that our prediction is based on an assumption of identical momentum distributions for antipartons and for partons as constituents of the physical proton. We have no evidence for such an assumption. If we think of the partons as quarks then the antiquark or antiparton distribution of a proton state may have very little relation to the parton distribution as observed in inelastic proton scattering. If we think of the proton as built of three quarks plus a background sea or glue of quark pairs then the antiquark distribution for this analysis should be correlated only to

that portion of the inelastic electron scattering that remains after the contribution of the simple three-quark model for the neutron and proton is removed. Evidence of the importance of this background sea or glue is now available from experiments on electron scattering from neutrons as well as protons [14]. It is clear from these experiments that the contribution of this sea or glue must be very important in order to explain the results. A further measure of the importance of the background sea comes from the normalization of the theoretical curve to the data in Fig. 15. We have used a relatively small value of $1/\lambda^2 \sim (1/2) - 1$ in (90) in order to adjust the calculated curve to the data. This value is in contrast to typical values of $1/(1/3)^2 = 9$ or $1/(2/3)^2 = 9/4$ associated with the quark model and suggests as in the analysis of the data [14] that the sea and the three quarks are both of comparable importance.

To paint the "real" picture of the proton's structure we shall need all the clues that come from massive lepton pair production in hadron–hadron collisions together with deep inelastic scattering results from neutrons and protons. The first step here is to verify the scaling law (62).

VI. Light Cone Behavior

In this final section we discuss briefly the possible role of singularities near the light cone in controlling the behavior of (49) and, through it, in determining the energy and mass dependence of this cross section. Arguments of this type have shed light on scaling behavior for the deep inelastic scattering process in the Bjorken limit in terms of singularities of almost equal time commutators. In (49) we are not computing a commutator but simply a product of currents. However as the momentum q carried by the current grows large one might argue that the dominant coordinate values in (49) will decrease so that the product $q \cdot x$ is finite. Contributions from other space-time regions will presumably be damped by the very rapid oscillations of $e^{iq\cdot x}$. Such an approach has been proposed and studied by Altarelli, Brandt, and Preparata [15] who in this way arrive at a different functional form than we have found in this work. Specifically our scaling result of (58),

$$\frac{d\sigma}{dQ^2} \sim \left(\frac{1}{Q^2}\right)^2 \mathscr{F}(\tau) \tag{92}$$

is replaced in their work by a form

$$\frac{d\sigma}{dQ^2} \sim \left(\frac{G_1(\tau)}{M_1{}^4} + \frac{G_2(\tau)}{M_2{}^2 Q^2}\right),$$

containing two scale factors M_1 and M_2 and two scale invariant functions $G_i(\tau)$

which can be further simplified if Regge pole behavior is assumed to dominate. Before commenting on this argument let us review how analogous ones have been applied to the study of almost equal time commutators in the deep inelastic process in the Bjorken limit [16].

In order to illustrate the sense in which $x^\mu \to 0$, i.e., how the interval decreases so that only the short distance behavior of $J_\mu(x)\, J_\nu(0)$ need be considered in (14) we find it convenient to work in the laboratory frame of the target proton

$$P^\mu = (M, 0).$$

For deep inelastic scattering in the Bjorken limit the photon momentum is to leading order

$$q^\mu \cong \nu \left(1, 0, 0, 1 + \frac{M}{\nu}\frac{1}{\omega}\right); \qquad \omega \equiv 2M\nu/Q^2 > 1,$$

and the exponential in (14) is

$$e^{iq\cdot x} \cong \exp\{i\nu(x_0 - x_3) - iMx_3/\omega\}. \tag{94}$$

The important space time interval, assumed to be the coordinate domain over which the integrand is not modulated by very rapid oscillations, is then

$$|\, x_0 - x_3 \,| \lesssim 1/\nu \to 0,$$
$$x_3\,,\, x_0 \lesssim \omega/M \qquad \text{i.e., finite,}$$

and by causality

$$0 < x_\mu x^\mu \lesssim \frac{\omega}{M\nu} - x_\perp{}^2 \lesssim \frac{\omega}{M\nu} \to 0. \tag{95}$$

Throughout the region defined by (95) and illustrated in Fig. 16 the scalar variables in the matrix element multiplying the exponent extend over a finite range also, i.e.,

$$0 \sim x_\mu x^\mu \to 0; \qquad \text{and} \quad x \cdot P = Mx_0 \sim \omega, \qquad \text{i.e., finite.}$$

With these constraints we see that the region along a finite segment of the light cone of length $\sim \omega/M$ and within an asymptotically vanishing invariant interval $\sim \sqrt{\omega/M\nu}$ in the time-like region about the light cone may be expected to determine the structure functions. By study of the current commutator and its singularities for a finite interval of length $\sim \omega/M$ along the light cone but only infinitesimally removed from it we can analyze the meaning of scaling in the Bjorken region.

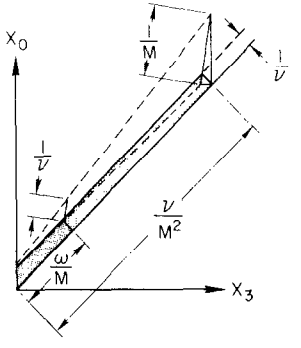

FIG. 16. The space-time region which gives the dominant contribution to the current commutator in electron–proton scattering in the Bjorken scaling limit (heavily shaded), and hadron–hadron scattering at high energies (lightly shaded). The first quadrant only is shown.

In contrast consider the space-time region of importance for high energy hadron–hadron total cross sections which can be obtained by unitarity from the imaginary part of (14) with q representing the four momentum of the incident nucleon in the laboratory system

$$q^\mu \cong \nu \left(1, 0, 0, 1 - \frac{M^2}{2\nu^2}\right).$$

In this case

$$e^{iq\cdot x} \cong \exp\left\{i\nu(x_0 - x_3) + i\frac{M^2}{2\nu}x_3\right\}, \tag{96}$$

and the important interval in contrast with (95) is

$$\begin{aligned} &|x_0 - x_3| \lesssim \frac{1}{\nu} \\ &x_3, x_0 \lesssim \frac{\nu}{M^2} \quad \text{i.e., unbounded and} \to \infty \text{ with} \quad \nu = \frac{s}{2M}, \end{aligned} \tag{97}$$

and

$$x_\mu x^\mu \lesssim \frac{1}{M^2} - x_\perp^2 \qquad \text{i.e., finite.}$$

For these processes which are usually studied in terms of Regge parameterization we are concerned with the region along an infinitely long segment of the light cone and of finite invariant width into the time-like region.

In this case we must know the behavior of the matrix element of the current commutators throughout a finite tube around the light cone but of infinitely long

length along the cone according to (97), unless the current operators themselves introduce a damping before

$$P \cdot x = Mx_3 \qquad \text{grows to} \sim \frac{\nu}{M} \to \infty$$

This difference in the space-time descriptions corresponds to the difference between the "wee" parton and the hard parton or impulse approximation regimes as we have earlier described them. In the Regge region the limit is always taken such that $\nu/M \to \infty$ whereas the corresponding parameter in the Bjorken limit is $\omega = (2M\nu/Q^2) = 1/x$ and is finite. Since the experimental value of a Regge pole parameterization of high energy processes has been established only for finite mass particles (real ones on their mass shells) entering the interaction we have no guide for continuing amplitudes between the Regge and impulse regimes. In order to relate the behavior of the matrix elements in either of these regimes, one finite and one asymptotically infinite, to singularities at the tip of the light cone

$$x^\mu \to 0; \quad \mu = 0,1,2,3$$

that have been analyzed by Wilson [17], added smoothness assumptions are required. In particular observed scaling in the Bjorken limit is used to select the correct behavior [16].

However when we turn to the massive pair formation in (49) we are no longer confined by the kinematics to the neighborhood of the light cone region; also since (49) contains a product of current operators, not a commutator, the matrix element does not vanish outside of the light cone for space-like separations. In contrast to the scattering where we could take the limit $q \to \infty$ in the laboratory frame we must here deal with the limiting process

$$q \to \infty \text{ and } s \to \infty \text{ so that } Q^2/s < 1 \text{ and finite}$$

The limit $q \to \infty$ with fixed P_1 and P_2 in (49) corresponds to

$$Q^2/s \to \infty$$

and is very far removed from the experimental regime of study and interest. But is is just this region of asymptotically large Q^2/s that we properly probe in a theoretical study by taking the $q^\mu \to \infty$ limit and expanding the matrix element about the origin in a power series as a function of $x_\mu x^\mu$ and $x \cdot (P_1 + P_2)$, as $x^\mu \to 0$. There is no assurance that such an expansion procedure works in the experimental region of interest. The relevance of the light cone $x_\mu x^\mu \sim 0$ for the analysis of massive mu-pair production as claimed by Alteralli et al. [15] depends on the assumed smooth behavior of the matrix element independent of whatever

may be its $s \to \infty$ limiting properties as we take $Q^2 \to \infty$ with $Q^2/s < 1$. For $Q^2 \to \infty$, with s fixed, the expansion about the light cone would be an elegant approach to this study, but for the experimentally accessible region, a very major extrapolation of the behavior of the matrix element is required. The mathematical conditions and assumptions for justifying the interchange of the limits $s \to \infty$ and $Q^2 \to \infty$ in Eq. (49) are discussed in Ref. [15].

CONCLUSION

We have described how the impulse approximation, whose roots lie in the *low energy* domain of atomic and nuclear bound states, finds a wide class of applications in the high energy electromagnetic and weak processes of the tightly bound systems forming single hadrons. For the latter we have to work in a properly chosen infinite momentum frame of the hadron system in order that the strong binding, as viewed in the laboratory frame, can be neglected as a consequence of the Lorentz dilatation of time scale. Only in such a system can we apply our intuition to working with almost free constituents—whatever and however many there may be—of the proton state. For atomic and nuclear systems the laboratory frame is a good working coordinate system since the binding of these systems is relatively much weaker.

Apart from this coordinate dependence of this approximation, atomic as well as nuclear processes and the deep inelastic hadronic processes are not very different conceptually. This analogy, although only qualitative, allows us to borrow the well-developed intuitive understanding of low energy nuclear physics as a guide to search for the clues of high energy or short distance substructure of the hadronic systems. Indeed, within the same framework of the impulse approximation we are able to give a unified treatment to the various deep inelastic processes involving one current, electromagnetic or weak: electron scattering, neutrino as well as antineutrino scattering, electron–positron annihilation into hadrons, massive lepton pair production in hadron–hadron collisions. Our goal has been to derive general scaling laws beyond the original accomplishment of Bjorken [4] who used the powerful, formal methods of dispersion theory and current algebra where they were applicable to the deep inelastic scattering. We have also related the different scaling processes in as model independent a way as possible, relating the electron scattering to electron–positron annihilation [5], neutrino scattering to antineutrino scattering [5], and electron scattering to neutrino scattering [5], massive pair production to electron scattering [2], and the threshold behavior of the structure function for electron scattering to the asymptotic behavior of the elastic nucleon form factors [7]. These relations are all empirically testable and probably will be confronted with experimental data in the near future. If they are found to be

correct they will lend strong support to the applicability and utility of the impulse approximation to these deep inelastic high energy processes involving the hard partons.

On the other hand validity of the scaling predictions, but not of the specific relations between the different processes, will bring the role of wee exchanges to the fore. As we have shown they do not effect the scaling arguments and to any finite order of calculation we can neglect the wee exchanges in relating electron scattering to e^+e^- pair annihilation or massive lepton pair production. However they may "exponentiate" to prominance when all orders are summed up [11] and provide an effective initial or final state interaction that will alter the specific predictions without destroying the validity of the impulse approximation.

The problem of wee parton exchange is obviously very difficult. Our treatment in this paper with respect to the "wees" is certainly not dynamical but kinematical. It is hoped that the recent high order calculations in certain field theory models will eventually lead to a more complete treatment of these wee partons, although undoubtedly that day is still not in sight [11, 18].

In addition to the role of the wee partons there are two other open issues not addressed by our approach:

(1) When and how does scaling set in with increasing Q^2, s, or $M\nu$?

(2) Where does the transverse momentum cutoff come from, and in detail how is it related to the conditions of vanishing wavefunction renormalization as we have conjectured [7, 5]?

REFERENCES

1. R. P. FEYNMAN, unpublished talks; *Phys. Rev. Lett.* **23** (1969), 1415; "Proceedings of the Third International Conference on High Energy Collisions at Stony Brook," Gordon and Breach Science Publishers, Inc., New York, 1969; J. D. BJORKEN AND E. PASCHOS, *Phys. Rev.* **185** (1969), 1975.
2. S. D. DRELL AND T. M. YAN, *Phys. Rev. Lett.* **25** (1970), 316.
3. S. D. DRELL, *in* "Proceedings of the International School of Physics "Ettore Majorana" Course 7," (A. Zichichi, Ed.), Academic Press, New York, to be published; proceedings of the International Conference on "Expectations for Particle Reactions at the New Accelerators" at the University of Wisconsin, Madison, Wisconsin, 1970.
4. J. D. BJORKEN, *Phys. Rev.* **179** (1969), 1547.
5. S. D. DRELL, D. J. LEVY, AND T. M. YAN, *Phys. Rev. Lett.* **22** (1969), 744. *Phys. Rev.* **187** (1969), 2159; *Phys. Rev. D.* **1** (1970), 1035; *Phys. Rev. D.* **1** (1970), 1617; T. M. YAN AND S. D. DRELL, *Phys. Rev. D* **1** (1970), 2402. The last four papers are referred to in text as Paper I, II, III, and IV, respectively.
6. J. H. CRISTENSON, G. S. HICKS, L. M. LEDERMAN, P. J. LIMON, B. G. POPE, AND E. ZAVATTINI, *Bull. Amer. Phys. Soc.* **15** (1970), 579; and the report submitted to the XVth International Conference on High Energy Physics, Kiev (1970). We thank Prof. Lederman for discussions of these experiments.

7. S. D. DRELL AND T. M. YAN, *Phys. Rev. Lett.* **24** (1970), 181.
8. We thank Prof. D. Yennie for a discussion which stimulated the consideration in this section.
9. J. BENECKE, T. T. CHOU, C. N. YANG, AND E. YEN, *Phys. Rev.* **188** (1969), 2159.
10. The fraction of the longitudinal momentum of the scattered parton is given by $x = Q^2/2M\nu$ which is finite.
11. S. J. CHANG AND T. M. YAN, Report No. SLAC-PUB-793, Stanford Linear Accelerator Center, Stanford Univ., Stanford, Calif., 1970.
12. These statements can be verified using the explicit representation of the Dirac matrices and spinors given in [5, Paper II Eqs. 6, 7, and 8].
13. T. D. LEE AND G. C. WICK, *Nucl. Phys. B.* **9** (1969), 209.
14. See report by R. E. Taylor to the XV International Conference on High Energy Physics, Kiev, USSR, August 1970 (SLAC-PUB-796); J. D. BJORKEN AND E. A. PASCHOS, *Phys. Rev.* **185** (1969), 1975.
15. G. ALTARELLI, R. BRANDT, AND G. PREPARATA, to be published.
16. See e.g., H. LEUTWYLER AND J. STERN, *Phys. Lett. B.* **31** (1970), 458; G. MACK, *Phys. Rev. Lett.* **25** (1970), 400; Y. FRISHMAN, to be published; R. JACKIW, R. VAN ROYEN, AND G. WEST, to be published.
17. K. WILSON, *Phys. Rev.* **179** (1969), 1499.
18. H. CHENG AND T. T. WU, *Phys. Rev. Lett.* **24** (1970), 1456; and references cited therein.